Detrimental incorporation of excess Cenp-A/Cid and Cenp-C into *Drosophila* centromeres is prevented by limiting amounts of the bridging factor Cal1

Ralf B. Schittenhelm[1,*], Friederike Althoff[1], Stefan Heidmann[2] and Christian F. Lehner[1,‡]

[1]Institute of Molecular Life Sciences, University of Zurich, CH-8057 Zurich, Switzerland
[2]Institute of Genetics, University of Bayreuth, D-95447 Bayreuth, Germany
*Present address: Institute of Molecular Systems Biology, ETH Zurich, CH-8093 Zurich, Switzerland
‡Author for correspondence (christian.lehner@imls.uzh.ch)

Accepted 4 July 2010
Journal of Cell Science 123, 3768-3779

doi:10.1242/jcs.067934

Summary

Propagation of centromere identity during cell cycle progression in higher eukaryotes depends critically on the faithful incorporation of a centromere-specific histone H3 variant encoded by *CENPA* in humans and *cid* in *Drosophila*. Cenp-A/Cid is required for the recruitment of Cenp-C, another conserved centromere protein. With yeast three-hybrid experiments, we demonstrate that the essential *Drosophila* centromere protein Cal1 can link Cenp-A/Cid and Cenp-C. Cenp-A/Cid and Cenp-C interact with the N- and C-terminal domains of Cal1, respectively. These Cal1 domains are sufficient for centromere localization and function, but only when linked together. Using quantitative in vivo imaging to determine protein copy numbers at centromeres and kinetochores, we demonstrate that centromeric Cal1 levels are far lower than those of Cenp-A/Cid, Cenp-C and other conserved kinetochore components, which scale well with the number of kinetochore microtubules when comparing *Drosophila* with budding yeast. Rather than providing a stoichiometric link within the mitotic kinetochore, Cal1 limits centromeric deposition of Cenp-A/Cid and Cenp-C during exit from mitosis. We demonstrate that the low amount of endogenous Cal1 prevents centromere expansion and mitotic kinetochore failure when Cenp-A/Cid and Cenp-C are present in excess.

Key words: Centromere, Kinetochore, Mitosis, Chromosome instability, Cal1

Introduction

The centromeric regions of chromosomes direct formation of kinetochores, which allow chromosome attachment to spindle microtubules. Centromeres and kinetochores are therefore of paramount importance for faithful propagation of genetic information (Santaguida and Musacchio, 2009). However, centromeric DNA sequences are not conserved (Vagnarelli et al., 2008). Most eukaryotes (including *Drosophila melanogaster* and humans) have regional centromeres with up to several megabases of repetitive DNA. Importantly, these repetitive sequences are neither necessary nor sufficient for centromere function, indicating that there is an epigenetic centromere specification (Vagnarelli et al., 2008).

A centromere-specific histone H3 variant (CenH3) is thought to be crucial for epigenetic centromere marking (Allshire and Karpen, 2008). CenH3 proteins are present in all eukaryotes (e.g. CENP-A in humans and Cid in *Drosophila*). They replace histone H3 in canonical nucleosomes or possibly variant complexes (Dalal et al., 2007; Mizuguchi et al., 2007; Camahort et al., 2009; Furuyama and Henikoff, 2009). Depletion of CenH3 results in a failure to localize most or all other centromere and mitosis-specific kinetochore proteins. Strong overexpression of *Drosophila* Cenp-A/Cid results in incorporation at ectopic chromosomal sites, which in part also assemble ectopic kinetochores during mitosis (Ahmad and Henikoff, 2002; Heun et al., 2006).

Ectopic kinetochores result in chromosome segregation errors and genetic instability. Ectopic CenH3 incorporation therefore must be prevented. Although still fragmentary, our understanding of the molecular mechanisms that regulate CenH3 incorporation is progressing rapidly (Allshire and Karpen, 2008; Torras-Llort et al., 2009). In proliferating cells, an additional complement of CenH3 needs to be incorporated during each cell cycle. In syncytial *Drosophila* embryos, this occurs during exit from mitosis (Schuh et al., 2007). Similar findings were made in human cells, where Cenp-A deposition occurs during late telophase and early G1 phase (Jansen et al., 2007). The number of factors shown to be required for normal CenH3 deposition is increasing rapidly, which suggests that there is an intricate control mechanism. Various and often dedicated chaperones (Hayashi et al., 2004; Furuyama et al., 2006; Dunleavy et al., 2009; Foltz et al., 2009), chromatin modifying and remodelling factors (Fujita et al., 2007; Maddox et al., 2007; Perpelescu et al., 2009), as well as other centromere components (Takahashi et al., 2000; Okada et al., 2006; Pidoux et al., 2009; Williams et al., 2009) are involved.

In *Drosophila*, Cenp-C is incorporated into centromeres concomitantly with Cenp-A/Cid (Schuh et al., 2007). High-resolution mapping with native *Drosophila* chromosomes has indicated that these two proteins do not have an identical localization within the kinetochore (Blower et al., 2002; Schittenhelm et al., 2007). Although these localization studies cannot exclude an association between subfractions of Cenp-A and Cenp-C, direct molecular interactions between these centromere proteins have not yet been reported. Recently, however, Cal1 has been identified in *Drosophila* and shown to be required for normal centromeric localization of Cenp-A/Cid and Cenp-C (Goshima et al., 2007; Erhardt et al., 2008). Moreover,

these three *Drosophila* centromere proteins can be co-immunoprecipitated from soluble chromatin preparations (Erhardt et al., 2008). Cal1 might therefore provide a physical link between Cenp-A/Cid and Cenp-C.

Here, we report that Cal1 has distinct binding sites for Cenp-A/Cid and Cenp-C. It can link these proteins together according to yeast three-hybrid experiments. However, the level of centromeric Cal1 is far lower than that of Cenp-A/Cid and Cenp-C. Cal1 therefore cannot function as a stoichiometric linker connecting each monomer or dimer of Cenp-C to Cenp-A within the centromere. But the low levels of Cal1 effectively protect cells against mitotic defects resulting from increased centromeric incorporation of excess Cenp-A/Cid and Cenp-C.

Results

cal1 is an essential gene required for centromere and kinetochore protein localization

RNAi-mediated knockdown of *cal1* has been shown to result in substantially diminished Cenp-A and Cenp-C levels at centromeres in *Drosophila* tissue culture cells (Goshima et al., 2007; Erhardt et al., 2008). For a genetic analysis of *cal1* function, we first characterized *cal1* alleles (Fig. 1A). The allele $cal1^{c03646}$ was confirmed to carry a *pBAC{PB}* insertion 69 bp upstream of the start codon within the predicted 5′ untranslated region. The *Mi{ET1}* insertion in $cal1^{MB04866}$ is within the second exon and disrupts the coding sequence after 361 of a total of 979 amino acids. Both insertions are associated with recessive lethality. They failed to complement each other, as well as the deficiency *Df(3R)Exel6176*, which deletes the *cal1* gene. The *gcal1-EGFP II.2* transgene, a genomic *cal1* fragment with the *EGFP* coding sequence inserted immediately before the stop codon (Fig. 1A), completely prevented the lethality of homo-, hemi- and transheterozygous $cal1^{MB04866}$ flies. Moreover, the rescued flies were found to be fertile. These findings demonstrate that *cal1* is an essential gene and that the Cal1-EGFP fusion provides all essential Cal1 functions.

To characterize the expression pattern of *cal1*, we used *gcal1-EGFP II.2* embryos. Microscopic analyses as well as immunoblotting experiments (supplementary material Fig. S1) indicated the presence of a maternal *cal1* contribution at the onset of embryogenesis, as well as a correlation of *cal1* expression with mitotic proliferation.

The maternal *cal1* contribution is expected to delay the onset of phenotypic abnormalities in *cal1* mutants. First abnormalities became apparent during stage 12. At this and later stages, abnormalities were largely restricted to the developing CNS (Fig. 1B). DNA staining revealed a lower number and a more irregular distribution of nuclei in the CNS of *cal1* mutants compared with sibling embryos. In addition, pyknotic nuclei as well as enlarged over-replicated nuclei were more frequently observed in the mutant CNS. Phospho-histone-H3-positive mitotic cells were also more frequent and often enlarged in the mutant CNS. The great majority of mutant progeny did not reach the larval stages (97%, n=100). Comparable observations were made with homo-, hemi- and transheterozygous embryos, suggesting that both alleles ($cal1^{MB04866}$ and $cal1^{c03646}$) result in a complete loss of gene function. The observed abnormalities in *cal1* mutants are consistent with the proposal that after exhaustion of the maternal *cal1* contribution, proliferating cells progress through aberrant mitoses with chromosome segregation errors resulting in aneuploidy and apoptosis.

Even before the onset of mitotic abnormalities, *cal1* homozygous mutant embryos displayed weaker anti-Cenp-A/Cid signals than sibling embryos (Fig. 1B). Later, when the abnormalities in the CNS became evident, Cenp-A/Cid could no longer be detected in *cal1* mutants. Moreover, the same results were also obtained with anti-Cenp-C, as well as with transgenes expressing EGFP fusions of Cenp-C, Spc105, Mis12, Nsl1, Spc25, Ndc80 and Nuf2 (supplementary material Fig. S2). The localization of all these centromere and kinetochore proteins requires Cal1. However, centromere localization of Cal1 was found to depend on

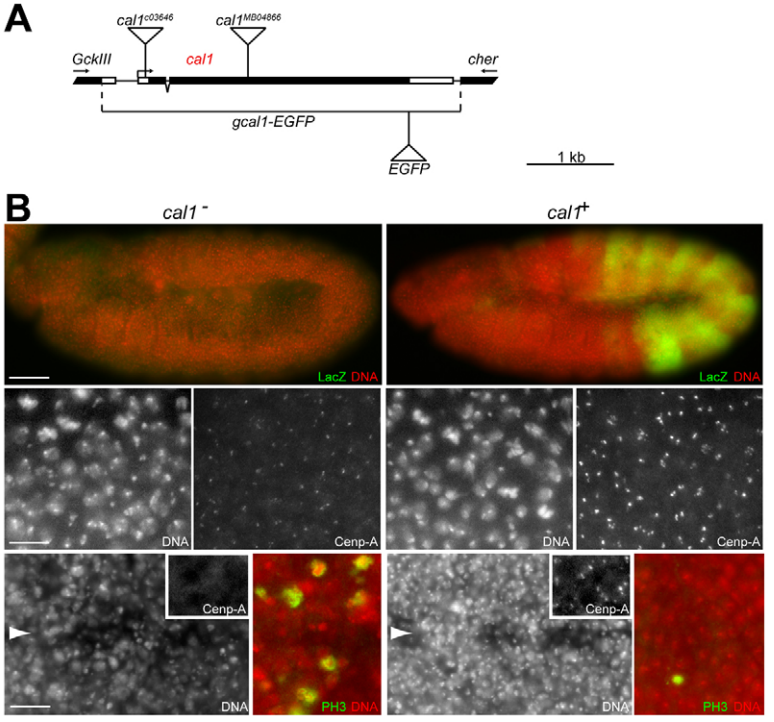

Fig. 1. Expression pattern and mutant phenotype of *cal1*. (**A**) Structure of wild-type and mutant *cal1* alleles. Boxes indicate exons; black fill, coding regions; and triangles, the *pBAC{PB}* and *Mi{ET1}* transposon insertions in $cal1^{c03646}$ and $cal1^{MB04866}$, respectively, as well as the EGFP insertion in the *gcal1-EGFP* transgene. Arrows indicate transcriptional start site and/or direction of transcription. (**B**) *cal1* mutant ($cal1^{-}$) and sibling control embryos ($cal1^{+}$) are shown on the left and right, respectively. Stage 11 is shown in the top and middle row, stage 14 in the bottom row. Embryos were collected from $cal1^{c03646}$/*TM3, Ubx-lacZ* parents, followed by labeling with a DNA stain (DNA) and antibodies against β-galactosidase for genotype determination (lacZ), against Cenp-A/Cid (Cenp-A) or phospho-histone H3 (PH3). The insets in the bottom row display anti-Cenp-A/Cid labeling in CNS cells at higher magnification. Arrowheads in the bottom row indicate the midline of the CNS. Scale bars: 50 µm (top), 6 µm (middle) and 11 µm (bottom).

Cenp-A/Cid and Cenp-C, but not on Spc105, Mis12 and Ndc80 complex components (supplementary material Fig. S2). Moreover, in contrast to initial descriptions (Heeger et al., 2005; Przewloka et al., 2007), quantification of anti-Cenp-A/Cid signals in Cenp-C mutant embryos confirmed (data not shown) that normal levels of centromeric Cenp-A/Cid depend on Cenp-C (Erhardt et al., 2008). All our findings in mutant embryos confirm and extend previous observations made after RNAi in *Drosophila* tissue cultures (Goshima et al., 2007; Erhardt et al., 2008). Cal1 clearly functions together with Cenp-A/Cid and Cenp-C in kinetochore assembly.

Cal1 promotes an interaction between Cenp-A/Cid and Cenp-C

Cal1, Cenp-A/Cid and Cenp-C can be co-immunoprecipitated (Erhardt et al., 2008). We analyzed whether Cal1 can interact simultaneously with Cenp-A/Cid and Cenp-C. Yeast two-hybrid (Y2H) assays clearly revealed an interaction of Cal1 with Cenp-A/Cid (Fig. 2A), but not with the kinetochore proteins Spc105, Mis12, Nsl1, Nnf1a, Bub1 or BubR1 (data not shown). The N-terminal region of Cal1 (residues 1–407) but not its middle (residues 392–722) and C-terminal (residues 699–979) regions were observed to interact with full-length Cenp-A/Cid (Fig. 2A). When the N-terminal tail or the histone fold domain of Cenp-A/Cid was assayed separately, no interactions with the N-terminal Cal1 region could be detected (data not shown). Y2H experiments also revealed an interaction between Cal1 and Cenp-C. The C-terminal regions of Cal1 (residues 699–979) and Cenp-C (residues 1009–1411) were found to interact (Fig. 2B). The interacting region within Cenp-C could be narrowed down to a smaller C-terminal subfragment (residues 1201–1411), which no longer included the Cenp-C box, a motif that is characteristic of all Cenp-C homologs (Fig. 2B). The C-terminal Cenp-C domain, which is sufficient for the Y2H interaction with Cal1, is similar in fungal and animal Cenp-C homologs (Talbert et al., 2004). It adopts a cupin fold and can mediate homodimerization (Cohen et al., 2008).

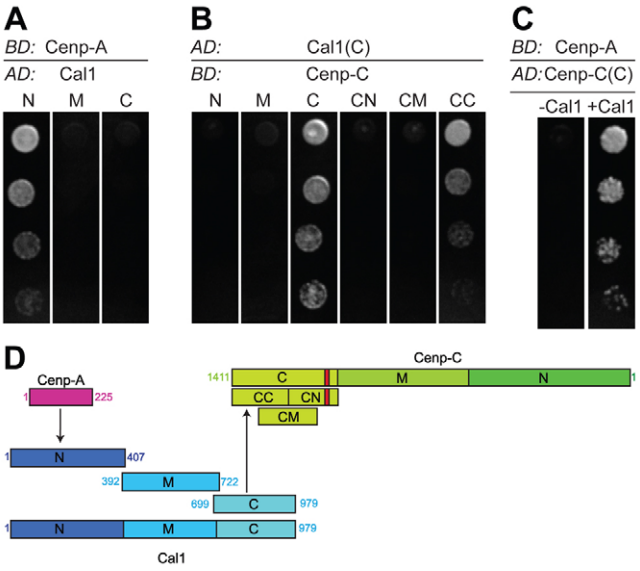

Fig. 2. Cal1 promotes interaction between Cenp-A/Cid and Cenp-C. (**A**) The N-terminal (N) but not the middle (M) or C-terminal (C) region of Cal1 interacts with Cenp-A/Cid. Full-length Cenp-A/Cid was fused to the DNA-binding domain (BD) and the Cal1 fragments to the transcriptional activation domain (AD) of Gal4 and interactions analyzed in Y2H experiments. (**B**) Y2H experiments reveal that the C-terminal domain of Cal1 [Cal1(C)] interacts specifically with C-terminal domains of Cenp-C [Cenp-C(C) and Cenp-C(CC)]. (**C**) Y3H experiments reveal that Cal1 expression results in an interaction between Cenp-A/Cid and Cenp-C(C). Cal1 expression is either repressed (–Cal1) or derepressed (+Cal1). (**D**) The observed protein interactions are indicated with arrows. Cal1 and Cenp-C were divided into N-terminal (N), middle (M) and C-terminal (C) domains. The C-terminal domain of Cenp-C was further split into three subregions (CN, CM, CC). The small red box indicates the position of the conserved Cenp-C box. Numbers indicate amino acid positions.

As Cenp-A/Cid and Cenp-C were observed to interact with distinct regions of Cal1, we evaluated whether Cal1 can bind to Cenp-A/Cid and Cenp-C simultaneously to form a trimeric complex (Fig. 2C). We generated a yeast strain constitutively expressing Cenp-A/Cid and Cenp-C(C) fused to the transcriptional activation and DNA-binding domain of Gal4, respectively. In addition, the strain allowed for regulated *cal1* expression. In the absence of *cal1* expression, we did not observe an interaction between Cenp-A/Cid and Cenp-C(C) (Fig. 2C). However, in the presence of *cal1* expression, we clearly observed a Cenp-A/Cid–Cenp-C(C) interaction (Fig. 2C). Control experiments demonstrated that the inducing growth conditions were unable to promote a Cenp-A/Cid–Cenp-C(C) interaction when the inducible *cal1* gene was absent (data not shown). The results of our yeast three-hybrid (Y3H) experiments therefore indicate that Cal1 can bridge Cenp-A/Cid and Cenp-C (Fig. 2D).

Centromere localization and function of Cal1 depends on both the Cenp-A/Cid- and Cenp-C-interacting regions

A perfect colocalization of Cenp-A/Cid, Cenp-C and Cal1 would be expected, if these proteins were present exclusively in a trimeric complex. Therefore, we carefully compared the localization of Cal1-EGFP with that of Cenp-A/Cid and Cenp-C in embryos and S2R+ cells expressing the *gcal1-EGFP* construct (supplementary material Fig. S3). Cal1-EGFP was observed at centromeres throughout the cell cycle. Importantly, during interphase, Cal1-EGFP signals, but not anti-Cenp-A/Cid and anti-Cenp-C signals, were also clearly enriched in and around the nucleolus. Our results therefore correspond to those described earlier (Erhardt et al., 2008) where antibodies against Cal1 were used. These results indicate that at least a fraction of Cal1 is not associated with Cenp-A/Cid and Cenp-C during interphase.

To evaluate which Cal1 domains contribute to localization, we generated constructs allowing expression of either the N-terminal, middle or C-terminal region fused to EGFP (Fig. 3A). The N- and C-terminal domains, which are sufficient for the interaction with either Cenp-A/Cid or Cenp-C, have been conserved more extensively during Drosophilid evolution than the middle region (Erhardt et al., 2008). None of the three Cal1 subregions was able to localize to the centromere in S2R+ cells (Fig. 3A). The middle, but not the terminal domains, became enriched in the nucleolus. To further define the requirements for Cal1 centromere localization, we generated constructs that allowed expression of different combinations of Cal1 domains (Fig. 3A). After expression of Cal1(N-M) or Cal1(M-C) we did not observe centromeric signals. However, these Cal1 fragments became enriched in the nucleolus (Fig. 3A), as expected because they contain the middle domain, which is sufficient for nucleolar localization. In agreement, Cal1(N-C), a Cal1 version lacking the middle domain, was not enriched in the nucleolus. Interestingly, however, this variant was found at the

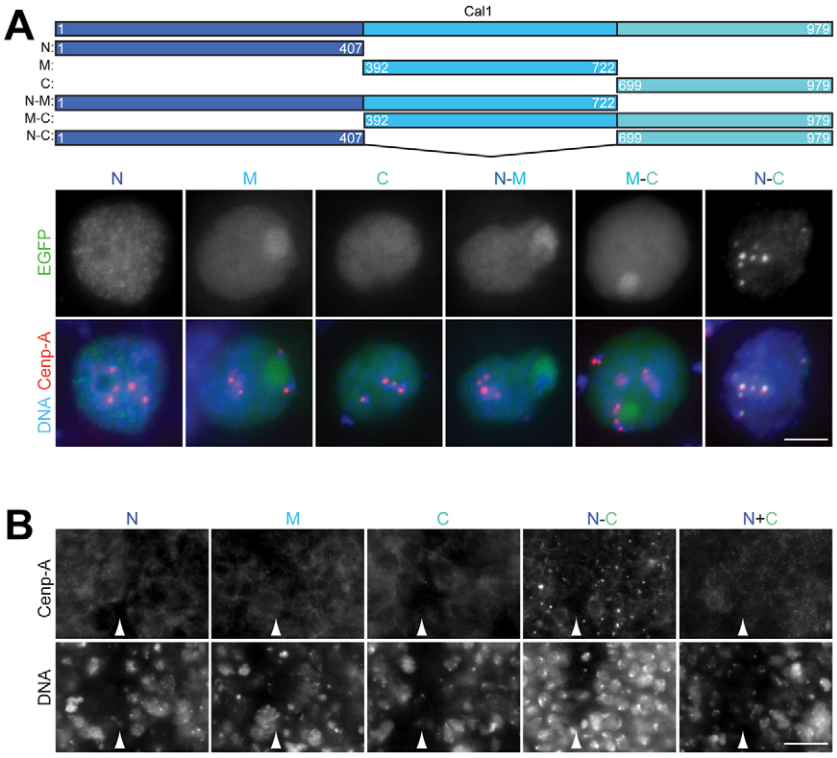

Fig. 3. Cal1 centromere localization and function require the linked Cenp-A/Cid and Cenp-C interacting regions. (**A**) Cal1 regions fused to EGFP were expressed in S2R+ cells after transient transfection with the illustrated constructs. Numbers indicate amino acid positions. Cells are labeled with an antibody against Cenp-A/Cid (Cenp-A) and a DNA stain (DNA). EGFP (EGFP) signals in representative nuclei are shown in the top row and merged images in the bottom row. Scale bar: 5 µm. (**B**) A covalent link between the N- and C-terminal domains of Cal1 is required to rescue the *cal1* mutant phenotype. *sca-GAL4* in combination with *UAS* transgenes was used for expression of different Cal1 regions in the central nervous system of *cal1* mutants. Embryos were fixed at stage 14 and labeled with a DNA stain (DNA), anti-Cenp-A/Cid (Cenp-A) and anti-β-galactosidase for genotype identification (not shown). Although the N-terminal (N), middle (M) and C-terminal (C) regions of Cal1 fail to restore centromeric Cenp-A/Cid localization and normal cell proliferation in *cal1* mutants, complete rescue is obtained with a Cal1 version with the N- and C-terminal regions directly linked (N-C). Simultaneous expression of the unlinked N- and C-terminal domains does not rescue the *cal1* mutant phenotype (N+C). Arrowheads indicate the midline of the CNS. Scale bar: 10 µm.

centromere throughout the cell cycle (Fig. 3A). Moreover, Y3H experiments indicated that Cal1(N-C) was still able to forge an interaction between Cenp-A/Cid and Cenp-C (data not shown). These findings suggest that Cal1 centromere localization depends on an interaction with Cenp-A/Cid and Cenp-C. Cal1 might be sequestered in the nucleolus when not in a complex with these centromeric proteins.

By expressing EGFP-tagged Cal1 variants in *cal1* mutant embryos, we evaluated to what extent the different Cal1 domains contribute to its function. Expression of the regions N, M or C (Fig. 3A) from *UAS* transgenes could be confirmed by the resulting EGFP signals (data not shown), but did not restore centromeric Cenp-A/Cid localization and normal cell proliferation in the CNS of *cal1* mutant embryos (Fig. 3B). However, expression of *UAS-cal1(N-C)-EGFP* prevented expression of the characteristic abnormalities in *cal1* mutant embryos (Fig. 3B). This rescue was just as effective as that with full-length Cal1 (*UAS-cal1-EGFP*, data not shown) and resulted in an apparently wild-type CNS. Moreover, ubiquitously expressed *UAS-cal1(N-C)-EGFP* allowed development of *cal1* mutants to the adult stage (data not shown). Importantly, simultaneous expression of *UAS-cal1(N)-EGFP* and *UAS-cal1(C)-EGFP* did not prevent the *cal1* mutant phenotype (Fig. 3B). In addition, EGFP signals were not centromeric, in contrast to those obtained with *UAS-cal1(N-C)-EGFP* (data not shown). Therefore, we conclude that centromere localization and function of Cal1 require the presence of its Cenp-A/Cid- and Cenp-C-interacting N- and C-terminal regions, which have to be linked, but not necessarily by its M region.

The amount of centromeric Cal1 is lower than that of Cenp-A/Cid and Cenp-C

The molecular interactions that are responsible for Cenp-C localization within the mitotic kinetochore are unknown. Human Cenp-C binds to DNA in vitro, although with very limited sequence preference (Yang et al., 1996; Sugimoto et al., 1997). Co-immunoprecipitation of human Cenp-C and Cenp-A has been reported (Erhardt et al., 2008; Trazzi et al., 2009), but others have failed to detect Cenp-C in Cenp-A nucleosomes (Hori et al., 2008). The co-immunoprecipitation data of Erhardt and colleagues (Erhardt et al., 2008) and our Y3H experiments are consistent with the notion that in *Drosophila*, Cal1 might function as a centromere component that stoichiometrically links Cenp-C to Cenp-A/Cid. To evaluate this possibility, we carefully quantified the centromeric amounts of these proteins. Wing imaginal discs of *Cenp-A/cid*-, *Cenp-C*- or *cal1*-null mutant larvae rescued by transgenes expressing functional EGFP fusions of these proteins were mounted next to *CSE4::EGFP* yeast cells (Fig. 4A). *CSE4* encodes the yeast Cenp-A homolog, which is thought to be present in two copies per centromere (Meluh et al., 1998; Collins et al., 2004). Accordingly, we used the clusters of the 16 centromeres in *CSE4::EGFP* anaphase or telophase cells (Fig. 4A; Joglekar et al., 2006) as an internal calibration standard for the quantification of Cenp-A/Cid-EGFP, Cenp-C-EGFP and Cal1-EGFP signal intensities in *Drosophila* centromeres. The measured Cse4-EGFP signal intensities were found to decrease with increasing distance of the centromere cluster from the coverslip (Fig. 4B), as described previously (Joglekar et al., 2006). In groups of cells with centromere clusters at similar focal positions, the s.d. values of the Cse4-EGFP signals were found to be lower than 36% of the average signal intensity. The EGFP signal intensities measured for the *Drosophila* centromere protein fusions that were expressed under the control of their own regulatory regions were also plotted against their average focal *z*-axis positions (Fig. 4C). The *y*-axis intercepts of linear regressions were used for comparison of the average amounts of different centromere proteins (Table 1). Moreover, the comparison of the EGFP signal intensities obtained in *Drosophila*

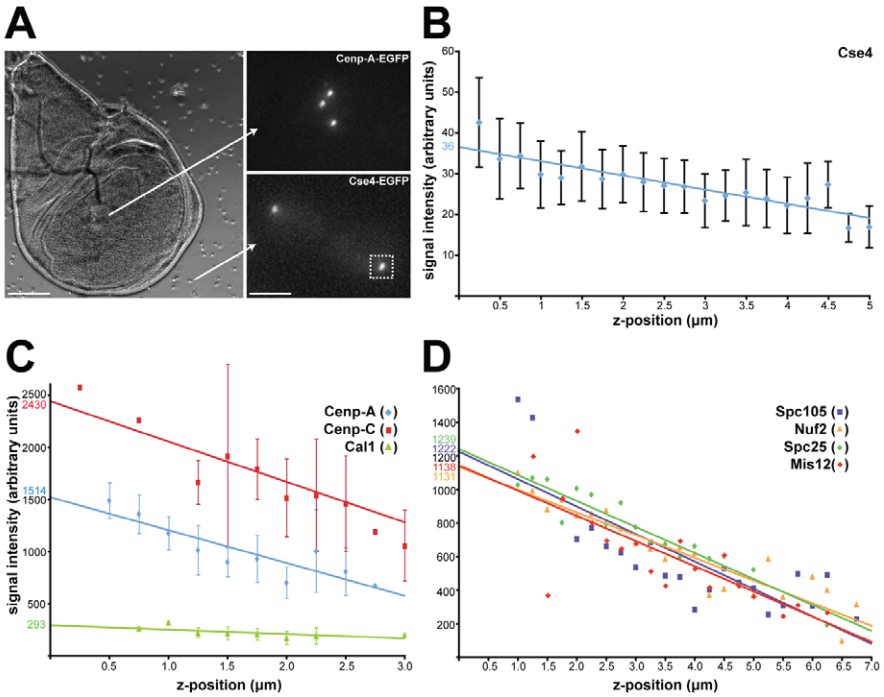

Fig. 4. Stoichiometry of *Drosophila* centromere and kinetochore proteins. (**A**) For EGFP signal quantification, *CSE4::EGFP* yeast cells were used as a reference (Joglekar et al., 2006) and mounted next to wing imaginal discs dissected from larvae homozygous for a null mutation and rescued by a transgene expressing an EGFP fusion of a particular *Drosophila* centromere or kinetochore protein. EGFP signals from *Drosophila* and yeast cells (e.g. Cenp-A/Cid-EGFP and Cse4-EGFP at late mitosis in the top and bottom panels on the right, respectively) were captured and quantified. Late mitotic yeast cells display two centromere clusters each containing 32 Cse4-EGFP protein copies (box). Scale bars: 100 µm (left), 3 µm (right). (**B**) As a reference, EGFP signal intensities of centromere clusters of late mitotic *CSE4::EGFP* cells were determined in all of the slides with different wing imaginal disc. Signal intensities show little variation between slides (data not shown), but they decrease with increasing focal depth of the centromere clusters (Joglekar et al., 2006). All the obtained values (664) are grouped into classes according to the focal depth of the centromere cluster. The mean signal intensities of the clusters in arbitrary units ± s.d. for each bin are plotted as a function of their *z* position. The *y*-axis intercept of a linear regression was used for comparison of Cse4-EGFP levels with those of *Drosophila* centromere and kinetochore proteins (Table 1). (**C**,**D**) The total centromeric signal intensity per cell quantified after expression of EGFP-fused centromere proteins (C: Cenp-A/Cid, Cenp-C or Cal1) or kinetochore proteins (D: Spc105, Mis12, Nuf2 or Spc25) in null mutant wing imaginal discs. Values are grouped according to the focal depth of the signals. The average signal intensity for each bin is plotted as a function of its *z* position. s.d. values are shown in C and omitted for clarity in D (but see supplementary material Fig. S4). *y*-axis intercepts of linear regressions were used for quantitative comparisons (see Table 1).

with those of Cse4-EGFP in yeast resulted in an estimate of the absolute protein copy numbers per centromere (Table 1). The accuracy of our quantifications was confirmed in competition experiments, where we observed the expected decrease in EGFP signal intensities when a given EGFP fusion protein was analyzed in a background that also expressed the untagged version of this protein from endogenous wild-type gene copies, rather than in a null-mutant background (supplementary material Fig. S4).

In case of Cal1-EGFP, specific signals were not only detected at the centromere as for Cenp-A/Cid-EGFP and Cenp-C-EGFP, but also in the nucleolus and weakly throughout the nucleus (supplementary material Fig. S4). Based on EGFP signal quantification, the centromeric, nucleolar and residual nuclear pools were estimated to comprise on average about 3.3%, 21% and 76%, respectively, of the total nuclear Cal1. Importantly, the amount of centromeric Cal1 was clearly far lower than that of Cenp-A/Cid and Cenp-C (Table 1). Our results therefore exclude models for centromeric Cenp-C localization where every Cenp-C monomer (or dimer) is stably linked via a single Cal1 protein to one or two copies of Cenp-A/Cid. The results of a comparison of the expression levels of the different EGFP fusion proteins (Cenp-A/Cid, Cenp-C, Cal1) by immunoblotting (supplementary material Fig. S5) was entirely consistent with this conclusion when taking into account the differential distribution of Cenp-A/Cid, Cenp-C and Cal1 into subnuclear regions (centromere, nucleolus, and elsewhere in the nucleus) as suggested by the quantitative in vivo imaging.

Quantitative imaging with imaginal discs was also used for a comparison of the amounts of the centromere proteins Cal1, Cenp-A/Cid and Cenp-C with those of the kinetochore proteins Spc105, Mis12, Spc25 and Nuf2 (Fig. 4D; Table 1). The levels of these kinetochore proteins were found to be all very similar and somewhat lower than the amounts of Cenp-A/Cid. The similar abundance measured for Spc25 and Nuf2 agrees with the established fact that they are stoichiometric components of the stable heterotetrameric Ndc80 complex (Santaguida and Musacchio, 2009). The comparison of the estimated numbers of protein copies per *Drosophila* kinetochore with those determined in yeast (Joglekar et al., 2006; Joglekar et al., 2008) indicated that the amounts of centromere and kinetochore proteins correlate rather with the number of kinetochore microtubules (1 in budding yeast, about 11 in *Drosophila*) (Winey et al., 1995; Maiato et al., 2006) than with the amount of centromeric DNA (125 bp in budding yeast, 420 kb in *Drosophila*) (Fitzgerald-Hayes et al., 1982; Sun et al., 1997).

Table 1. *Drosophila* centromere and kinetochore protein levels

Protein	Amount at centromere or kinetochore (arbitrary units)	Copy number per kinetochore[b]	Copy number per kMT[c]	Copy number of yeast homolog per kMT[d]
Cenp-A/Cid	1514[a]	84	7.6	2
Cenp-C	2430[a]	135	12.3	1–2
Cal1	293[e]/46[f]	2.5	0.23	Homolog?
Spc105	1222[g]	68	6.2	5
Mis12	1138[g]	63	5.7	5
Spc25	1239[g]	69	6.3	8
Nuf2	1131[g]	63	5.7	8

[a]Signals determined in interphase cells. In case of Cenp-C, signals were also quantified in prometaphase and metaphase cells where they were found to be comparable with the interphase value, as expected (Schuh et al., 2007).
[b]By comparison with the average Cse4-EGFP signal intensity, which was found to be 36 arbitrary units for a cluster of 16 kinetochores. Moreover, each kinetochore is assumed to contain two Cse4-EGFP molecules.
[c]Based on the assumption of 11 kMTs per *Drosophila* kinetochore (Maiato et al., 2006).
[d]Data from (Joglekar et al., 2006). Note that a budding yeast kinetochore binds a single kMT.
[e]Sum of centromeric and nucleolar Cal1-EGFP signals in interphase.
[f]Estimate for centromeric Cal1-EGFP signals in interphase.
[g]Signals determined in prometaphase and metaphase cells. In case of Mis12, signals were also quantified in interphase cells where they were found to be threefold lower than in mitosis. Centromeric signals cannot be detected during interphase in case of Spc105, Spc25 and Nuf2.

Interdependency between Cal1, Cenp-A/Cid and Cenp-C limit centromere expansion in combination with cell cycle control

Cenp-A/Cid deposition needs to be carefully controlled because the CenH3 variants of the CENP-A family have a crucial role in defining the epigenetic mark that specifies centromere identity in regional centromeres (Allshire and Karpen, 2008). In principle, the interdependence of centromeric Cenp-A/Cid, Cenp-C and the low levels of Cal1 might provide robust control of centromeric Cenp-A/Cid amounts and could effectively protect cells against the consequences of accidental unbalanced Cenp-A/Cid excess. However, previous studies have demonstrated that overexpression of Cenp-A/Cid is sufficient to cause ectopic incorporation all along the chromosome and consequential mitotic defects (Van Hooser et al., 2001; Heun et al., 2006; Moreno-Moreno et al., 2006). The massive overexpression applied in these studies (70-fold) (Heun et al., 2006), which is rather unlikely to occur in physiological conditions, even accidentally, might have over-run negative regulation. Therefore, we applied more limited overexpression in *Drosophila* embryos (up to fourfold; supplementary material Fig. S6), to evaluate the role of Cenp-A/Cid, Cenp-C and Cal1 interdependency in centromere confinement of these proteins.

Overexpression was achieved with the *prd-GAL4* driver, which directs *UAS* transgene expression in alternating segmental stripes within the embryonic epidermis (Fig. 5A). Overexpression starts during embryonic cell cycle 14. Embryos were fixed and analyzed 3 hours later, when the majority of the epidermal cells are in G2 of cycle 16. Intervening stripes that do not express *prd-GAL4* were used as internal controls.

Interestingly, when *UAS-Cenp-A/cid* was expressed, we could detect at most a marginal increase in the intensity of centromeric anti-Cenp-A/Cid signals in the *prd-GAL4* expressing stripes (Fig. 5B,C). However, when *UAS-Cenp-A/cid* and *UAS-cal1-EGFP* were simultaneously overexpressed, we observed a highly significant increase in centromeric Cenp-A/Cid (Fig. 5B,C; $P<0.001$, Student's *t*-test). *UAS-cal1-EGFP* without concomitant *UAS-Cenp-A/cid* expression did not result in increased centromeric anti-Cenp-A/Cid signals (Fig. 5B,C). Quantification of centromeric Cal1-EGFP fluorescence indicated that coexpression of *UAS-Cenp-A/cid* and *UAS-cal1-EGFP* resulted in slightly higher levels than when *UAS-cal1-EGFP* was expressed alone (Fig. 5B,C). We conclude that moderate overexpression of Cenp-A/Cid does not lead to increased centromeric Cenp-A/Cid levels because Cal1 levels are limiting. Similarly, Cenp-A levels limit centromeric Cal1 levels. These findings are consistent with the proposal that deposition of Cenp-A/Cid at the centromere requires complex formation with Cal1, probably by direct interaction as suggested by our Y2H experiments.

To analyze the interplay of Cenp-A/Cid and Cal1 with Cenp-C, we quantified centromeric anti-Cenp-C signals. As our Y3H experiments had indicated that Cal1 can form a bridge between Cenp-A and Cenp-C, these three proteins might be incorporated into the centromere as a stoichiometric stable complex. Accordingly, the increased Cenp-A/Cid and Cal1-EGFP incorporation observed after simultaneous overexpression is expected to be accompanied by a parallel increase in centromeric Cenp-C. However, we did not detect such an increase (Fig. 5C). This finding confirms that centromeres are not assembled by multimerization of stable persisting complexes of Cal1, Cenp-A/Cid and Cenp-C.

Expression of *UAS-Cenp-C* provided additional confirmation for the notion that centromeric accumulation of Cenp-A/Cid and Cenp-C are not necessarily coupled. Although *UAS-Cenp-C* expression clearly resulted in an increase of centromeric Cenp-C (Fig. 5C; $P<0.001$, Student's *t*-test), it was not paralleled with a comparable increase in centromeric Cenp-A (Fig. 5C). The increased centromeric anti-Cenp-C signals observed after *UAS-Cenp-C* expression suggest that the Cenp-C binding sites within the centromere are not saturated at the endogenous Cenp-C expression level. However, because *UAS-Cenp-C* expression caused increased anti-Cenp-C signals not only at the centromere, but also throughout the cell (data not shown), the centromeric Cenp-C binding sites appear to become limiting when Cenp-C is overexpressed.

Although our findings indicated that centromeric accumulation of Cenp-C is not necessarily coupled to that of Cal1-Cenp-A/Cid, simultaneous overexpression of all three centromere proteins clearly revealed synergism. In this case, maximal centromeric signals were obtained. Signals were significantly higher than after overexpression of *UAS-Cenp-A/cid*, *UAS-Cenp-C* and *UAS-cal1-EGFP* individually or in pairs (Fig. 5B; $P<0.01$ for all comparisons, Student's *t*-test). These findings are consistent with the suggestion that Cal1-mediated transient interactions between Cenp-A/Cid and Cenp-C support their centromeric deposition.

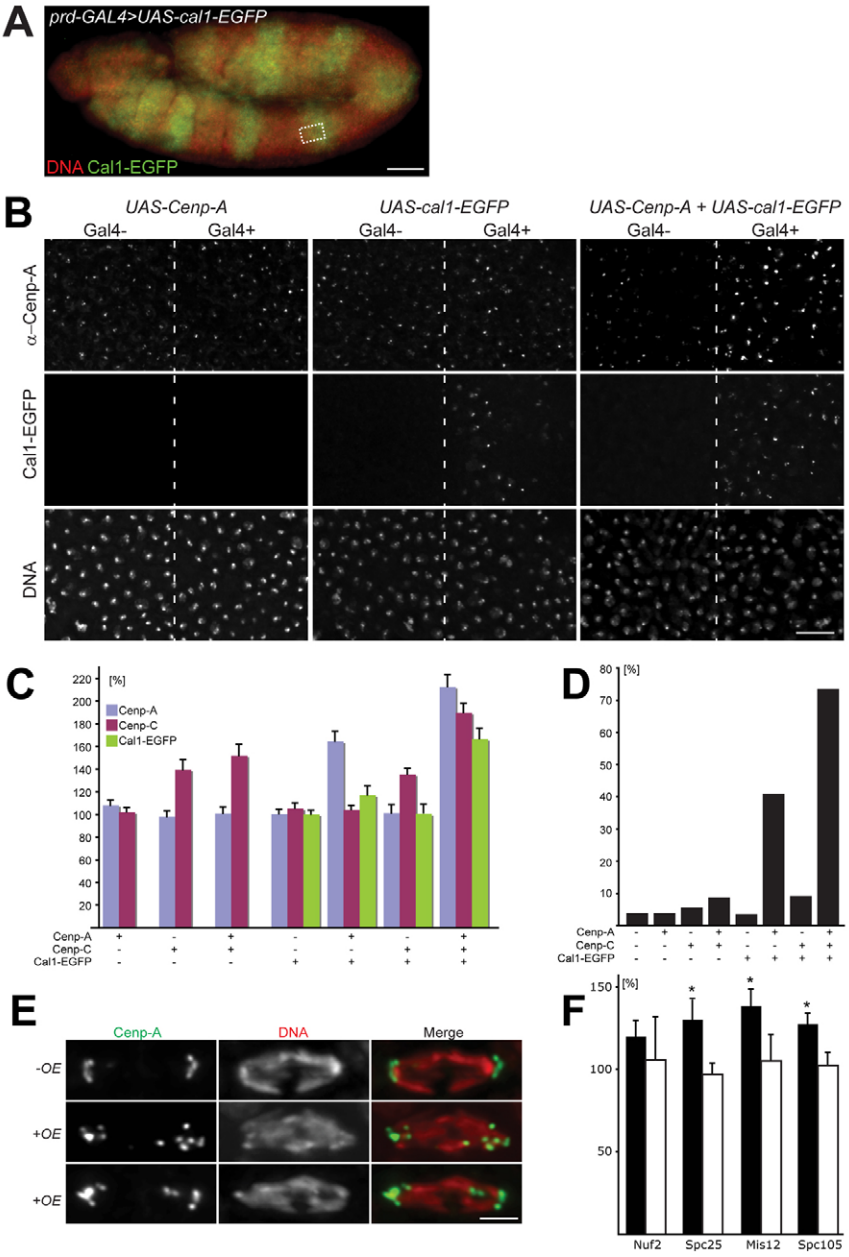

Fig. 5. Interdependence of Cenp-A/Cid, Cenp-C and Cal1 limits centromere expansion and genetic instability. (**A**) *prd-GAL4* was used to direct expression of *UAS-cal1-EGFP*, *UAS-Cenp-A/cid* and *UAS-Cenp-C* individually or in combination in alternating segmental stripes as illustrated by Cal1-EGFP signals (green) and DNA staining (red) in a stage 11 embryo expressing *UAS-cal1-EGFP*. The dashed rectangle indicates the position of the regions shown in B. Scale bar: 50 µm. (**B**) *prd-GAL4* was used for striped expression of *UAS-Cenp-A/cid* (left), *UAS-cal1-EGFP* (middle), or both these *UAS* transgenes (right). Epidermal regions are shown with dashed lines indicating the border between domains with ($Gal4^{+}$) and without ($Gal4^{-}$) expression of *UAS* transgenes. Top, anti-Cenp-A/Cid (α-*Cenp-A*); middle row, Cal1-EGFP signals; bottom, DNA. Increased centromeric Cenp-A/Cid and Cal1-EGFP signals result after co-overexpression, but not after individual overexpression of *UAS-cal1-EGFP* and *UAS-Cenp-A/cid* (see also C). Scale bar: 15 µm. (**C**) Centromeric signal intensities obtained after labeling with either anti-Cenp-A/Cid or anti-Cenp-C were quantified in embryos with *prd-GAL4*-driven overexpression of *UAS* transgenes in stripes (see A and B). Signal intensities observed in stripes without *UAS* transgene expression are set as 100%. Bars indicate relative centromeric signal intensities within the *UAS* transgene expressing stripes (average intensity with s.e.m., $n>5$ embryos). Cal1-EGFP signals were compared with those obtained within stripes expressing only *UAS-cal1-EGFP*, which were set as 100%. The type(s) of *UAS* transgenes expressed is indicated below the bars. (**D**) Percentage of abnormal late mitotic figures observed in the embryonic epidermis at the stage of mitosis 16 after α*4tub-GAL4-VP16*-driven expression of the different *UAS* transgenes. (**E**) Characteristic anaphase figures observed in the embryonic epidermis at the stage of mitosis 16 in either control embryos (–OE, top) or after α*4tub-GAL4-VP16*-driven expression of *UAS-Cenp-A/cid*, *UAS-Cenp-C* and *UAS-cal1-EGFP* (+OE, middle and bottom). Embryos were labeled with anti-Cenp-A/Cid (Cenp-A) and a DNA stain (DNA). Scale bar: 4 µm. (**F**) Various kinetochore proteins (Nuf2, Spc25, Mis12 and Spc105) were expressed as EGFP fusions from transgenes under control of the endogenous regulatory regions in embryos where *prd-GAL4* was also driving co-expressing *UAS-cal1*, *UAS-Cenp-A/cid* and *UAS-Cenp-C* (black bars) or only *UAS-cal1* and *UAS-Cenp-A/cid* (white bars). EGFP signals in kinetochores of prometaphase and metaphase cells were quantified. Those observed in stripes without *UAS* transgene expression were set as 100%. Bars indicate relative signal intensities within the stripes expressing the *UAS* transgene (average intensity with s.e.m., $n>5$ embryos). The increased signal intensities of Spc25, Mis12 and Spc105 in stripes expressing the *UAS* transgene are significant (*$P<0.05$, Student's *t*-test).

The observed increase in the centromeric levels of Cenp-A/Cid, Cenp-C and Cal1-EGFP after simultaneous *prd-GAL4*-driven overexpression did not appear to result in severe mitotic defects. Abnormal mitotic figures at the stage of mitosis 16 were rarely observed and chromosomal incorporation of Cenp-A/Cid, Cenp-C and Cal1-EGFP outside the centromere was not detected. However, clear mitotic defects resulted (Fig. 5D) when we used maternal α*4tub-GAL4-VP16*, which drives almost twofold higher expression than *prd-GAL4* (data not shown). The strongest defects were caused by simultaneous expression of all three centromere proteins. Milder defects were already apparent after combined expression of *UAS-Cenp-A/cid* and *UAS-cal1-EGFP* (Fig. 5D). By contrast, all other combinations or individual expression of the *UAS* transgenes did not result in a distinct enrichment of abnormal mitotic figures (Fig. 5D). Expression of *UAS* transgenes during eye and wing development further confirmed that the combined overexpression of the three centromere proteins is far more deleterious than individual overexpression (supplementary material Fig. S7).

To address how α*4tub-GAL4-VP16*-driven simultaneous expression of *UAS-Cenp-A/cid*, *UAS-Cenp-C* and *UAS-cal1-EGFP* affects progression through mitosis, we characterized the mitotic abnormalities in further detail. The most prominent defects observed in fixed embryos were abnormal anaphase and telophase figures with chromatin bridges containing lagging centromeres (Fig. 5E). Ectopic Cenp-A/Cid incorporation throughout the chromosome arm regions was rarely detectable in these abnormal mitotic figures. Focal ectopic Cenp-A/Cid incorporation within a chromosome arm might in principle lead to multicentric chromosomes and thereby explain the observed chromosome bridges with lagging centromeres after simultaneous overexpression of Cenp-A/Cid, Cenp-C and Cal1-EGFP. Therefore, we counted the number of kinetochores in mitotic cells. Even in wild-type controls, we were unable to detect all of the 16 centromeres as distinct Cenp-A/Cid or Cenp-C foci in every mitotic cell. Apart from the occasional immediate proximity of kinetochores, accessibility problems resulting in low anti-Cenp-A/Cid or anti-Cenp-C signals specifically during prometaphase and metaphase further impaired kinetochore identification. Therefore, we used EGFP-Nuf2-expressing embryos for kinetochore counting. Moreover, we determined kinetochore counts after expression of *prd-GAL4*-directed *UAS* transgenes in adjacent control and overexpressing regions to eliminate effects of fixation variability. Analyses after *prd-GAL4*-driven overexpression were possible because mitotic abnormalities were frequent at the stage of mitosis 16 when *UAS-cal1* was used instead of the *UAS-cal1-EGFP* transgene insertion selected for the initial experiments (Fig. 5A–C). The stronger effect of *UAS-cal1* presumably reflects transgene position effects on expression levels or absence of the EGFP tag which might be slightly deleterious. Despite the occurrence of late-mitotic figures with lagging centromeres within the overexpressing regions, the number of discrete kinetochore spots was not significantly increased within these regions (10.3±1.6 EGFP-Nuf2 spots compared with 10.7±1.6 spots in the intervening stripes; $n>50$ cells from more than 10 different embryos). These results suggest that ectopic kinetochores are not the primary cause for the mitotic abnormalities resulting from co-overexpression of Cal1, Cenp-A/Cid and Cenp-C.

As ectopic kinetochores could not be observed, we determined whether increased centromeric Cal1, Cenp-A/Cid and Cenp-C was accompanied with increased levels of kinetochore proteins. Transgenes expressing EGFP fusions of a given kinetochore protein (Nuf2, Spc25, Mis12 or Spc105) under the control of their normal cis-regulatory regions were used in combination with *prd-GAL4*-driven simultaneous overexpression of the three centromere proteins Cal1, Cenp-A/Cid and Cenp-C in stripes. The EGFP signals in the kinetochores of mitotic cells were found to be slightly but consistently enhanced within the overexpressing stripes (Fig. 5F). This enhancement was less extensive than that of Cal1, Cenp-A/Cid and Cenp-C (compare Fig. 5C and F). However, in these experiments the kinetochore proteins were not overexpressed from *UAS* transgenes in contrast to Cal1, Cenp-A/Cid and Cenp-C. The comparatively mild increase of kinetochore proteins observed after co-overexpression of Cal1, Cenp-A/Cid and Cenp-C might therefore reflect limiting kinetochore protein expression levels. Interestingly, when only Cal1 and Cenp-A/Cid but not Cenp-C was overexpressed, we were unable to detect a statistically significant increase in kinetochore protein levels (Fig. 5F), suggesting that the observed mitotic defects (Fig. 5D) do not depend on increased kinetochore protein levels.

To analyze the consequences of simultaneous overexpression of Cal1, Cenp-A/Cid and Cenp-C on the dynamics of progression through mitosis, we performed in vivo imaging with embryos expressing histone H2Av-mRFP and Cenp-A/Cid-EGFP in addition to *UAS-cal1*, *UAS-Cenp-A/cid* and *UAS-Cenp-C* (Fig. 6; supplementary material Movies 1 and 2). First abnormalities were already apparent during mitosis 15. Compared with controls, which did not overexpress the centromeric proteins, chromosome congression into a metaphase plate was always slower (2- to 8-fold; mean 3.7-fold; $n=8$ cells from two embryos) and metaphase prolonged (3- to 18-fold; mean 10-fold; $n=10$ cells from two embryos) except in one cell. Although chromosome segregation during anaphase appeared to be normal in about half of the cases ($n=11$ cells from two embryos), the other half displayed subtle to strong abnormalities. Characteristically, these abnormalities consisted in lagging centromeres (Fig. 6A, data not shown). During mitosis 16, these same mitotic defects were even more pronounced (Fig. 6A). The distances between sister kinetochores in metaphase plates were found to be scattered over a wider range after co-overexpression of Cal1, Cenp-A/Cid and Cenp-C (Fig. 6B). Collectively, our analyses of the observed mitotic abnormalities suggest that increased levels of centromeric Cal1, Cenp/Cid and Cenp-C compromise kinetochore function during mitosis.

Normally, centromere loading of Cenp-A/Cid and Cenp-C occurs during and depends on exit from mitosis (Jansen et al., 2007; Schuh et al., 2007). To evaluate whether the observed increase in centromere protein levels that results from simultaneous overexpression of Cal1, Cenp-A/Cid and Cenp-C also depends on progression through mitosis, we performed experiments in *string(stg)/cdc25* mutant embryos where cells remain arrested in G2 phase of cycle 14 (Edgar and O'Farrell, 1989). After overexpression of Cal1, Cenp-A/Cid and Cenp-C in these G2-arrested cells, we did not observe increased anti-Cenp-A/Cid and Cenp-C signals at centromeres (supplementary material Fig. S8). However, some ectopic accumulation throughout the cells was apparent. By contrast, an increased centromeric signal, at the expense of distributed signals was clearly obtained after progression through a successful mitosis, which was triggered with the help of a heat-inducible *hs-stg* transgene in *stg* mutant embryos overexpressing Cal1, Cenp-A/Cid and Cenp-C. We conclude that increased incorporation of Cal1, Cenp-A/Cid and Cenp-C into centromeres requires both overexpression and progression through

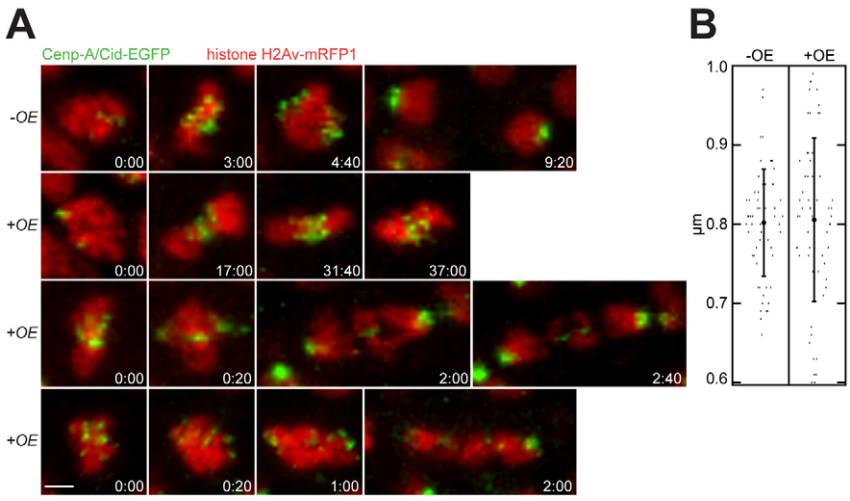

Fig. 6. Co-overexpression of Cenp-A/Cid, Cenp-C and Cal1 results in a metaphase delay. (**A**) Time-lapse in vivo imaging of the sixteenth round of mitosis in embryos expressing Cenp-A/Cid-EGFP and histone H2Av-mRFP1 with (+OE) or without (–OE) simultaneous α*4tub-GAL4-VP16*-driven overexpression of *UAS-cal1*, *UAS-Cenp-A/cid* and *UAS-Cenp-C*. The time (minutes:seconds) indicated in each frame is given relative to the start of prophase (first and second row) or the end of metaphase (third and fourth row), which was set to zero. Compared with controls (–OE; first row), embryos overexpressing Cal1, Cenp-A/Cid and Cenp-C (+OE; second row) show a delay in chromosome congression and during metaphase. Subsequent chromosome segregation is normal in only 50% of the observed anaphases (not shown). The other half display subtle or strong abnormalities, as illustrated in the third and fourth row. Scale bar: 3 µm. (**B**) The distances (in µm) between sister kinetochores in metaphase plates of embryos with (+OE) or without (–OE) α*4tub-GAL4-VP16*-driven overexpression of *UAS-cal1*, *UAS-Cenp-A/cid* and *UAS-Cenp-C* are illustrated in box plots. Each dot represents one sister kinetochore pair. Mean values (with s.d.) are indicated by the two larger dots. After co-overexpression of Cal1, Cenp-A/Cid and Cenp-C, the distances between sister kinetochores scatter over a wider range.

mitosis. Moreover, the excess levels of Cal1, Cenp-A/Cid and Cenp-C that were not yet incorporated into the centromere did not lead to mitotic defects during the *hs-stg*-induced mitosis.

Discussion

Drosophila Cal1 has been identified recently because its knockdown in cultured cells results in a loss of Cenp-A/Cid and Cenp-C from centromeres and a failure of chromosome alignment and segregation during mitosis (Goshima et al., 2007; Erhardt et al., 2008). Here, we demonstrate that Cal1 is a crucial component of the important regulatory mechanisms that prevent an excessive incorporation of Cenp-A/Cid and Cenp-C into centromeres and consequential chromosome mis-segregation.

cal1 is an essential gene that is expressed specifically in mitotically proliferating cells. To provide its function, the protein product needs its N-terminal domain, which interacts with Cenp-A/Cid, as well as its C-terminal domain, which interacts with Cenp-C. By contrast, the most rapidly diverging middle region of Cal1 seems to be of lesser importance because expression of the N-C version, which lacks the M domain, is sufficient to prevent the characteristic defects in *cal1* mutant embryos. The obvious functionality of the N-C version also emphasizes the importance of the centromeric localization of Cal1. The complete Cal1 protein is observed not only at the centromere, but also in the nucleolus. The M region is both sufficient and required for nucleolar localization. However, because this M domain is not required for *cal1* mutant rescue, the significance of the nucleolar Cal1 localization remains unclear.

Rescue of *cal1* mutants is not observed when the N- and C-terminal domains of Cal1 are expressed without a covalent linkage. The ability to recruit Cenp-A/Cid and Cenp-C into a complex, as clearly evidenced by our yeast three-hybrid experiments, is therefore likely to be crucial for Cal1 function. Co-immunoprecipitation of Cal1, Cenp-A/Cid and Cenp-C has previously indicated that these components can associate in vivo (Erhardt et al., 2008). However, our quantification of protein levels, which is largely dependent on the accuracy of our EGFP signal quantifications, demonstrates that Cenp-C is not exclusively anchored to centromeric chromatin via persistent and stoichiometric Cal1-mediated links to Cenp-A/Cid. Centromeric Cal1 levels are more than 40-times lower than those of Cenp-A/Cid and Cenp-C.

The centromeric amount of Cal1 is also far lower than that of the other kinetochore components that we have quantified (Spc105, Spc25, Nuf2). Interestingly, per kinetochore, the copy numbers of these components appear to be scaling well with the number of kinetochore microtubules (kMTs) when comparing our results from *Drosophila* with those described for budding and fission yeast (Joglekar et al., 2006; Joglekar et al., 2008). Spc25 and Nuf2 are constituents of the heterotetrameric Ndc80 complex, which binds directly to kMTs (Santaguida and Musacchio, 2009). Eight copies of the Ndc80 complex are thought to bind a single kMT to the budding yeast kinetochore (Joglekar et al., 2006). In *Drosophila*, where the number of kMTs per kinetochore appears to be around 11 (Maiato et al., 2006), about seven copies appear to be present per kMT according to our quantification. Our quantification of kinetochore proteins fits very well with the notion that the kinetochores of higher eukaryotes might be composed of several copies of a module that is present in one copy in budding yeast. By contrast, the centromere proteins Cenp-A and Cenp-C are scaling less well with the number of kMTs. The increased complexity of lateral co-ordination within animal kinetochores and of epigenetic specification of centromere identity might explain the higher relative amount of centromere proteins apparent in *Drosophila*. Despite this relative increase, centromeric Cenp-A/Cid allows packaging of only about 5% of the centromeric DNA in *Drosophila* under the assumption that Cenp-A/Cid nucleosomes

wrap about 200 bp of a 200 kb centromere (Sun et al., 1997; Allshire and Karpen, 2008).

Although our quantifications exclude the notion that Cal1 functions as a stable stoichiometric linker of Cenp-A/Cid and Cenp-C in mitotic kinetochores, our overexpression experiments provide further support for a role as a centromere protein-loading factor (Erhardt et al., 2008). Moreover, our experiments reveal additional layers of regulation that prevent excess incorporation of centromere proteins within the centromeric region. They also indicate that such excess incorporation is highly detrimental to kinetochore function. Previous work in *Drosophila* has demonstrated that strong overexpression of Cenp-A/Cid (about 70-fold) can lead to ectopic kinetochore formation (Heun et al., 2006). However, almost all Cenp-A/Cid that is incorporated ectopically within the chromosome arm regions is degraded rapidly (Moreno-Moreno et al., 2006), which is also observed in yeast (Collins et al., 2004). Here, we show that the limiting amounts of Cal1 provide additional, highly efficient protection against excessive chromosomal incorporation of Cenp-A/Cid. After bypassing this protection by Cal1 overexpression, even low levels of Cenp-A/Cid overexpression (about 2.5-fold) result in increased incorporation into centromeres (about 1.6-fold). When, in addition to Cal1 and Cenp-A/Cid, Cenp-C is also mildly co-overexpressed (about 3.5-fold), the levels of centromeric Cenp-A/Cid are further increased (about 2-fold) along with those of Cal1 and Cenp-C. Importantly, co-overexpression of these centromere proteins resulted not only in increased centromeric levels, but also in severe mitotic defects.

Although other interpretations are not excluded, our findings strongly suggest that the mitotic defects observed after overexpression of Cal1 and Cenp-A/Cid, and even more strongly when Cenp-C was also overexpressed, reflect the consequence of the increase in the centromeric levels of these proteins. The increase in centromeric levels of centromere proteins was accompanied by a significant increase in kinetochore proteins (Spc105 and the Mis12 and Ndc80 complex) but only to a very limited extent and only when all three centromere proteins were co-expressed. The increased amounts of centromeric Cenp-A/Cid observed after co-expression of Cal1 and Cenp-A/Cid, which were not accompanied by a statistically significant increase in kinetochore protein levels, might therefore be sufficient to disturb the spatial organization of the kinetochore, leading to inefficient chromosome congression, spindle checkpoint hyperactivation and chromosome segregation defects in anaphase.

Our experiments in *stg* mutant embryos, demonstrate that co-overexpression of centromeric proteins during interphase is not sufficient to cause excess centromeric incorporation, consistent with the previously demonstrated dependence of centromeric deposition of Cenp-A/Cid and Cenp-C on exit from mitosis (Schuh et al., 2007). Indeed, forcing progression through mitosis (by *hs-stg* induction) was observed to be sufficient to cause centromeric deposition of the overexpressed proteins. Moreover, the fact that the excess centromere proteins that were not yet incorporated into the centromere did not disturb the *hs-stg* induced mitosis, further supports our suggestion that the mitotic defects observed after co-expression of centromeric proteins depend on excessive incorporation into the centromere.

The severe mitotic defects observed after co-overexpression of Cal1, Cenp-A/Cid and Cenp-C emphasize the importance of careful control of centromere protein deposition. Several levels of control are effective. The interdependence of Cal1, Cenp-A/Cid and Cenp-C functions in conjunction with cell cycle control to prevent detrimental excessive centromeric incorporation. The cell cycle regulators cyclin A, Rca1/Emi1 and Fzr/Cdh1 have recently been implicated in the control of deposition of Cenp-A/Cid and Cenp-C at the centromere (Erhardt et al., 2008). How these and possibly additional cell cycle regulators control centromere protein deposition has yet to be clarified.

A possible scenario for centromere protein deposition in *Drosophila* might include a release of nucleolar Cal1 at the onset of mitosis, followed by conversion into a form that associates with non-centromeric soluble Cenp-A/Cid during exit from mitosis. After binding of soluble Cenp-A/Cid to the N-terminal domain of Cal1, its C-terminal domain might become exposed so that it can bind to centromeric Cenp-C and promote Cenp-A/Cid transfer onto the neighboring centromeric chromatin and thereby indirectly also additional Cenp-C deposition.

The mechanisms and the extent of control of centromeric Cenp-A deposition appear to have evolved. In fission yeast, overexpression of Cenp-A/Cid alone is sufficient to obtain excess centromeric Cenp-A/Cnp1, and this excess does not result in increased kinetochore protein levels (Joglekar et al., 2008). Spreading of Cenp-A within centromeric chromatin has also been clearly demonstrated in human cells after mild overexpression of Cenp-A (Lam et al., 2006). Mitotic defects were not detected in this case, perhaps because of the very limited increase in centromeric Cenp-A. Cal1 homologs from non-Drosophilid genomes have not yet been identified so far. Conversely, with the exception of Cenp-C, homologs of the 15 components of the vertebrate centromere chromatin-associated network (CCAN), which is related to the yeast Ctf19 and Sim4 complexes, have not been revealed in Drosophilid genomes, neither by thorough bioinformatic analyses (Meraldi et al., 2006) nor by genome-wide RNAi screens (Goshima et al., 2007; Erhardt et al., 2008). The CCAN seems also to be absent in *C. elegans* (Cheeseman et al., 2004; Sonnichsen et al., 2005; Gassmann et al., 2008). It is conceivable therefore that Cal1 is a functional analog of the CCAN, which has also been implicated in Cenp-A loading (Okada et al., 2006). However, because the evolutionary sequence conservation of centromere and kinetochore components is generally very low, it remains a possibility that Cal1 homologs also exist and function in centromere loading of human Cenp-A and Cenp-C.

Materials and Methods

Fly strains

cal1^{c03646} (Thibault et al., 2004), *cal1*^{MB04866} (Metaxakis et al., 2005) and *Df(3R)Exel6176* (Parks et al., 2004) were obtained from the Bloomington *Drosophila* Stock Center. *gEGFP-cal1* lines were generated using *ΦC31*-mediated germline transformation (Bischof et al., 2007) and *UAS-cal1*, *UAS-cal1-EGFP*, *UAS-cal1(N)-EGFP*, *UAS-cal1(M)-EGFP*, *UAS-cal1(C)-EGFP*, *UAS-cal1(N-C)-EGFP* and *gcal1-EGFP* with *pP{CaSpeR-4}* constructs (details provided upon request).

The wing imaginal discs analyzed for the quantification of centromere and kinetochore proteins fused to EGFP (Schuh et al., 2007; Schittenhelm et al., 2007; Schittenhelm et al., 2009) were from larvae with the following genotypes:
w; cid*$^{T12\text{-}1}$*/cid*$^{T22\text{-}4}$*; P{w*$^{+}$*, gcid-EGFP-cid} III.2*
w; P{w*$^{+}$*, giEGFP-Cenp-C} II.1; FRT82B Cenp-C*^{prl41}
w; P{w*$^{+}$*, gcal1-EGFP}II.2; cal1* ^{MB04866}
w; P{w*$^{+}$*, gSpc105-EGFP} II.1; Spc105*^{1}
w; gMis12-EGFP II.2; Mis12*^{f03756}*/Df(3L)BSC27*
w; P{w*$^{+}$*, gSpc25-EGFP} II.1; Spc25*^{c00064}
w; Nuf2*^{ex50}*; P{w*$^{+}$*, gEGFP-Nuf2} III.1.*

For the analyses in stg mutant embryos, we crossed *w*; P{w*$^{+}$*, UAS-cal1-EGFP} II.1/CyO, P{ry*$^{+}$*, ftz-lacZ}; P{w*$^{+}$*, UAS-Cenp-A/cid} III.5, P{w*$^{+}$*, UAS-Cenp-C} III.1, stg*^{7B}*/TM3, Sb, P{w*$^{+}$*, Ubx-lacZ}* males with either *w*; stg*^{7B}*, e, P{w*$^{+}$*, da-GAL4} G32/TM3, Sb, P{w*$^{+}$*, Ubx-lacZ}* or *w*; stg*^{7B}*, e, P{w*$^{+}$*, hs-stg} 3.1, P{w*$^{+}$*, da-GAL4} G32/TM3, Sb, P{w*$^{+}$*, Ubx-lacZ}* females.

Yeast two- and three-hybrid assays

Protein–protein interactions were analyzed essentially as described (Jäger et al., 2004). For Y3H analyses, the yeast strain MaV203 (Invitrogen) was cotransformed with a *pBridge-cal1* and a *pGADT7* construct and plated on *SD-Leu-Trp* selective drop-out medium. Colonies were transferred to appropriate selective drop-out medium plates (SD-Leu-Trp-Ura and SD-Leu-Trp-His) with or without methionine. *cal1* expression from the *pBridge* construct is controlled by the P_{Met25} promoter and occurs only in the absence of methionine.

Transfections, immunoblotting and immunolabeling

Transfection of S2R+ cells was conducted with the FuGeneHD Transfection Reagent (Roche) essentially as described (Schittenhelm et al., 2007). Immunofluorescence and DNA labeling of S2R+ cells and fixed embryos was also done essentially as described (Pandey et al., 2005; Schittenhelm et al., 2007). Rabbit antibodies against EGFP (1:3000), Cenp-A/Cid (Jäger et al., 2005), Cenp-C (Heeger et al., 2005) and Spc105 (Schittenhelm et al., 2009), as well as mouse anti-α-tubulin (DM1A, 1:50,000, Sigma) and anti-lamin Dm0 (ADL67.10, 1:200) were used for immunoblotting.

For quantification of centromeric anti-Cenp-A/Cid and anti-Cenp-C signal intensities (Fig. 5B,C), we crossed *prd-GAL4/TM3, Sb, P{w$^+$, Ubx-lacZ}* females to males carrying various *UAS* transgenes individually or in combination (*UAS-Cenp-A/cid III.5*, *UAS-Cenp-C III.1* and *UAS-cal1-EGFP II.1*). Embryos were collected for 2 hours and aged for 5 hours at 25°C before fixation and immunolabeling with rabbit anti-Cenp-A/Cid or anti-Cenp-C, mouse anti-β-galactosidase (for genotype determination) and Hoechst 33258 (DNA stain).

For quantification of kinetochore protein levels (Fig. 5F), we crossed females carrying *prd-GAL4* recombined with a transgene driving expression of a kinetochore protein fused to EGFP under the control of the endogenous regulatory region (*gMis12-EGFP III.1*, *gSpc105-EGFP III.1*, *gEGFP-Nuf2 III.1* or *gSpc25-EGFP III.1*) over *TM3, Sb, P{w$^+$, Ubx-lacZ}* to males carrying various *UAS*-transgenes individually or in combination (*UAS-Cenp-A/cid III.5*, *UAS-Cenp-C III.1* and *UAS-cal1 II.1*).

Quantification of signal intensities in embryos with *prd-GAL4* expressing and non-expressing regions was performed after acquisition of stacks with a 63×/1.4 oil-immersion objective and 250 nm spacing from the epidermal region of the second and third thoracic and the first abdominal segment. Within this imaged region, *prd-GAL4* drives expression in the outer but not in the middle segment. A Colibri light source (Zeiss) with a 470 nm light emitting diode was used for EGFP excitation with reproducible and temporally stable intensity. The stacks were deconvolved (Huygens Remote Manager v1.0 beta 2; Montpellier RIO Imaging) and subsequently converted into maximum projections using ImageJ.

For quantification of anti-Cenp-A/Cid and anti-Cenp-C signals, stacks with 12 sections were acquired from six different embryos for each genotype. A rectangle from the middle region that does not express *prd-GAL4* was first selected. Subsequently, the average intensity of the centromeric pixels within the selected rectangle was determined after applying a threshold to eliminate non-centromeric signals. Moreover, the average pixel intensity of non-centromeric pixels was determined and defined as background within the selected rectangle. Subtraction of this background from the intensity of centromeric pixels resulted in our measure of centromeric signal intensity within the middle internal control region that does not express *prd-GAL4*. Thereafter, rectangles from the flanking regions that express *prd-GAL4* were selected, followed again by thresholding to select centromeric pixels. To arrive at our measure of centromeric signal intensities within the *prd-GAL4*-expressing regions, we subtracted the background determined in the middle internal control region. By subtracting the background determined in the middle internal control region from the intensity of the non-centromeric pixels within the *prd-GAL4*-expressing regions, we arrived at a measure for the non-centromeric excess of the overexpressed centromere protein.

For Cal1-EGFP signal quantification, we were unable to use the intervening middle region as an internal control because *UAS-cal1-EGFP* was only expressed within the *prd-GAL4*-expressing regions, Therefore, we determined centromeric GFP signal intensities by applying a threshold to select the centromeric pixels within the *prd-GAL4*-expressing regions followed by subtraction of the background, which was obtained by averaging signal intensities of the non-centromeric pixels. The values obtained for all six embryos of a given genotype were averaged. The average obtained with embryos expressing only *UAS-cal1-EGFP* was set to 100% to arrive at the bars presented in Fig. 5C.

Quantification with or without prior deconvolution resulted in identical ratios of centromeric signal intensities between *prd-GAL4*-expressing and non-expressing regions in case of the anti-Cenp-A/Cid staining. In case of anti-Cenp-C and Cal1-EGFP, higher non-centromeric signals precluded a reliable, exclusive segmentation of centromeric signals without prior deconvolution. However, in these cases, quantification of individually selected centromeres using the two-square method with local background correction (see below) also resulted in very similar results, irrespective of prior deconvolution.

For quantification of EGFP-tagged kinetochore components, we acquired stacks with 12 sections from at least seven different embryos. Individual prometaphase or metaphase cells in the maximum projections were selected consecutively by two concentric squares (side length, 50 pixel and 55 pixels, respectively). The total pixel intensity of each square was determined and the average pixel intensity within the region encircled by the larger, but not by the smaller square was determined as local background. The average background pixel intensity integrated over the smaller square was subtracted from the total pixel intensity within the smaller square to yield the kinetochore signal intensity of a cell.

In vivo imaging

Embryos obtained from a cross of *α4tub-GAL4-VP16, gHis2AvD-mRFP II.2*, *gcid-EGFP-cid II.1 / CyO*, *P{ry$^+$, ftz-lacZ}* females with *UAS-cal1 II.1; UAS-Cenp-A/cid III.5*, *UAS-Cenp-C III.1* males were analyzed by in vivo imaging essentially as described (Pandey et al., 2005) at the stage when epidermal cells progress through the fifteenth (4–5 hours) or sixteenth (6.5–7.5 hours) round of mitosis. Time-lapse imaging was performed with an Olympus FV1000 system. Stacks (four sections, 250 nm spacing) were acquired at intervals of 20 seconds using a 60× oil-immersion objective and converted to maximum projections. Embryos from *α4tub-GAL4-VP16, gHis2AvD-mRFP II.2*, *gcid-EGFP-cid II.1 / CyO*, *P{ry$^+$, ftz-lacZ}* females crossed against *w^1* males were analyzed for control.

For the comparison of the levels of *Drosophila* centromere and kinetochore proteins fused to EGFP with those of Cse4-EGFP in yeast, we dissected wing imaginal discs from third instar wandering stage larvae in Schneider's *Drosophila* medium (Invitrogen). The imaginal discs were mounted in phosphate-buffered saline (PBS) on a coverslip previously coated with yeast cells of strain KBY7006 (*S. cerevisiae* 473a CSE4-GFP:KAN; (Joglekar et al., 2006) kindly provided by Kerry Bloom (University of North Carolina, Chapel Hill, NC). Yeast cells from a fresh overnight culture grown in YPD at 25°C were resuspended in PBS after sedimentation and a wash in H_2O. The suspension was spread on a coverslip coated with concanavalin A for about 5 minutes. Immediately before mounting freshly dissected wing imaginal discs, a region in the center of the coverslip was wiped dry. Imaginal discs were mounted in this region with their peripodial membranes facing the cover slip. Stacks (20–27 sections, 250 nm spacing) were acquired using a 63×/1.4 oil immersion objective and a Zeiss Cell Observer HS. The stacks were converted into maximum projections using ImageJ. For Cse4-EGFP signal quantification, individual centromere clusters of anaphase or telophase cells were selected by two concentric squares (side length, 20 and 22 pixels, respectively) and centromeric signal intensity was determined after background subtraction as described above for kinetochore EGFP fusion proteins. For quantification of EGFP-tagged centromere and kinetochore components in imaginal wing discs, at least 40 individual cells from more than three wing discs per genotype were also selected by two concentric squares (side length, 50 and 55 pixels, respectively) followed by determination of centromeric signal intensity after background subtraction as described above.

We would like to thank Romanas Chaleckis for assistance during the Y2H experiments, Sebastian Heeger for initial characterization of Cenp-A/Cid and Cenp-C overexpression, Alf Herzig for the *stg^{7B}, hs-stg, da-GAL4* stock, Johannes Bischof and Konrad Basler for sharing the unpublished cloning vector *pattB*, as well as Brigitte Jaunich and Sina Niebur for technical help. This work was supported by grants of the Swiss National Science Foundation (SNF 3100A0-120276/1) and the Deutsche Forschungsgemeinschaft (DFG He 2354/2-4).

Supplementary material available online at
http://jcs.biologists.org/cgi/content/full/123/21/3768/DC1

References

Ahmad, K. and Henikoff, S. (2002). Histone H3 variants specify modes of chromatin assembly. *Proc. Natl. Acad. Sci. USA* **99**, 16477-16484.

Allshire, R. C. and Karpen, G. H. (2008). Epigenetic regulation of centromeric chromatin: old dogs, new tricks? *Nat. Rev. Genet.* **9**, 923-937.

Bischof, J., Maeda, R. K., Hediger, M., Karch, F. and Basler, K. (2007). An optimized transgenesis system for Drosophila using germ-line-specific phiC31 integrases. *Proc. Natl. Acad. Sci. USA* **104**, 3312-3317.

Blower, M. D., Sullivan, B. A. and Karpen, G. H. (2002). Conserved organization of centromeric chromatin in flies and humans. *Dev. Cell* **2**, 319-330.

Camahort, R., Shivaraju, M., Mattingly, M., Li, B., Nakanishi, S., Zhu, D., Shilatifard, A., Workman, J. L. and Gerton, J. L. (2009). Cse4 is part of an octameric nucleosome in budding yeast. *Mol. Cell* **35**, 794-805.

Cheeseman, I. M., Niessen, S., Anderson, S., Hyndman, F., Yates, J. R., 3rd, Oegema, K. and Desai, A. (2004). A conserved protein network controls assembly of the outer kinetochore and its ability to sustain tension. *Genes Dev.* **18**, 2255-2268.

Cohen, R. L., Espelin, C. W., De Wulf, P., Sorger, P. K., Harrison, S. C. and Simons, K. T. (2008). Structural and functional dissection of Mif2p, a conserved DNA-binding kinetochore protein. *Mol. Biol. Cell* **19**, 4480-4491.

Collins, K. A., Furuyama, S. and Biggins, S. (2004). Proteolysis contributes to the exclusive centromere localization of the yeast Cse4/CENP-A histone H3 variant. *Curr. Biol.* **14**, 1968-1972.

Dalal, Y., Wang, H., Lindsay, S. and Henikoff, S. (2007). Tetrameric structure of centromeric nucleosomes in interphase Drosophila cells. *PLoS Biol.* **5**, e218.

Dunleavy, E. M., Roche, D., Tagami, H., Lacoste, N., Ray-Gallet, D., Nakamura, Y., Daigo, Y., Nakatani, Y. and Almouzni-Pettinotti, G. (2009). HJURP is a cell-cycle-

dependent maintenance and deposition factor of CENP-A at centromeres. *Cell* **137**, 485-497.
Edgar, B. A. and O'Farrell, P. H. (1989). Genetic control of cell division patterns in the Drosophila embryo. *Cell* **57**, 177-183.
Erhardt, S., Mellone, B. G., Betts, C. M., Zhang, W., Karpen, G. H. and Straight, A. F. (2008). Genome-wide analysis reveals a cell cycle-dependent mechanism controlling centromere propagation. *J. Cell Biol.* **183**, 805-818.
Fitzgerald-Hayes, M., Buhler, J. M., Cooper, T. G. and Carbon, J. (1982). Isolation and subcloning analysis of functional centromere DNA (CEN11) from Saccharomyces cerevisiae chromosome XI. *Mol. Cell. Biol.* **2**, 82-87.
Foltz, D. R., Jansen, L. E., Bailey, A. O., Yates, J. R., 3rd, Bassett, E. A., Wood, S., Black, B. E. and Cleveland, D. W. (2009). Centromere-specific assembly of CENP-a nucleosomes is mediated by HJURP. *Cell* **137**, 472-484.
Fujita, Y., Hayashi, T., Kiyomitsu, T., Toyoda, Y., Kokubu, A., Obuse, C. and Yanagida, M. (2007). Priming of centromere for CENP-A recruitment by human hMis18alpha, hMis18beta, and M18BP1. *Dev. Cell* **12**, 17-30.
Furuyama, T. and Henikoff, S. (2009). Centromeric nucleosomes induce positive DNA supercoils. *Cell* **138**, 104-113.
Furuyama, T., Dalal, Y. and Henikoff, S. (2006). Chaperone-mediated assembly of centromeric chromatin in vitro. *Proc. Natl. Acad. Sci. USA* **103**, 6172-6177.
Gassmann, R., Essex, A., Hu, J. S., Maddox, P. S., Motegi, F., Sugimoto, A., O'Rourke, S. M., Bowerman, B., McLeod, I., Yates, J. R., 3rd et al. (2008). A new mechanism controlling kinetochore-microtubule interactions revealed by comparison of two dynein-targeting components: SPDL-1 and the Rod/Zwilch/Zw10 complex. *Genes Dev.* **22**, 2385-2399.
Goshima, G., Wollman, R., Goodwin, S. S., Zhang, N., Scholey, J. M., Vale, R. D. and Stuurman, N. (2007). Genes required for mitotic spindle assembly in Drosophila S2 cells. *Science* **316**, 417-421.
Hayashi, T., Fujita, Y., Iwasaki, O., Adachi, Y., Takahashi, K. and Yanagida, M. (2004). Mis16 and Mis18 are required for CENP-A loading and histone deacetylation at centromeres. *Cell* **118**, 715-729.
Heeger, S., Leismann, O., Schittenhelm, R., Schraidt, O., Heidmann, S. and Lehner, C. F. (2005). Genetic inteactions of Separase regulatory subunits reveal the diverged Drosophila Cenp-C homolog. *Genes Dev.* **19**, 2041-2053.
Heun, P., Erhardt, S., Blower, M. D., Weiss, S., Skora, A. D. and Karpen, G. H. (2006). Mislocalization of the Drosophila centromere-specific histone CID promotes formation of functional ectopic kinetochores. *Dev. Cell* **10**, 303-315.
Hori, T., Amano, M., Suzuki, A., Backer, C. B., Welburn, J. P., Dong, Y., McEwen, B. F., Shang, W. H., Suzuki, E., Okawa, K. et al. (2008). CCAN makes multiple contacts with centromeric DNA to provide distinct pathways to the outer kinetochore. *Cell* **135**, 1039-1052.
Jäger, H., Herzig, B., Herzig, A., Sticht, H., Lehner, C. F. and Heidmann, S. (2004). Structure predictions and interaction studies indicate homology of separase N-terminal regulatory domains and Drosophila THR. *Cell Cycle* **3**, 182-188.
Jäger, H., Rauch, M. and Heidmann, S. (2005). The Drosophila melanogaster condensin subunit Cap-G interacts with the centromere-specific histone H3 variant CID. *Chromosoma* **113**, 350-361.
Jansen, L. E., Black, B. E., Foltz, D. R. and Cleveland, D. W. (2007). Propagation of centromeric chromatin requires exit from mitosis. *J. Cell Biol.* **176**, 795-805.
Joglekar, A. P., Bouck, D. C., Molk, J. N., Bloom, K. S. and Salmon, E. D. (2006). Molecular architecture of a kinetochore-microtubule attachment site. *Nat. Cell Biol.* **8**, 581-585.
Joglekar, A. P., Bouck, D., Finley, K., Liu, X., Wan, Y., Berman, J., He, X., Salmon, E. D. and Bloom, K. S. (2008). Molecular architecture of the kinetochore-microtubule attachment site is conserved between point and regional centromeres. *J. Cell Biol.* **181**, 587-594.
Lam, A. L., Boivin, C. D., Bonney, C. F., Rudd, M. K. and Sullivan, B. A. (2006). Human centromeric chromatin is a dynamic chromosomal domain that can spread over noncentromeric DNA. *Proc. Natl. Acad. Sci. USA* **103**, 4186-4191.
Maddox, P. S., Hyndman, F., Monen, J., Oegema, K. and Desai, A. (2007). Functional genomics identifies a Myb domain-containing protein family required for assembly of CENP-A chromatin. *J. Cell Biol.* **176**, 757-763.
Maiato, H., Hergert, P. J., Moutinho-Pereira, S., Dong, Y., Vandenbeldt, K. J., Rieder, C. L. and McEwen, B. F. (2006). The ultrastructure of the kinetochore and kinetochore fiber in Drosophila somatic cells. *Chromosoma* **115**, 469-480.
Meluh, P. B., Yang, P., Glowczewski, L., Koshland, D. and Smith, M. M. (1998). Cse4p is a component of the core centromere of Saccharomyces cerevisiae. *Cell* **94**, 607-613.
Meraldi, P., McAinsh, A. D., Rheinbay, E. and Sorger, P. K. (2006). Phylogenetic and structural analysis of centromeric DNA and kinetochore proteins. *Genome Biol.* **7**, R23.
Metaxakis, A., Oehler, S., Klinakis, A. and Savakis, C. (2005). Minos as a genetic and genomic tool in Drosophila melanogaster. *Genetics* **171**, 571-581.
Mizuguchi, G., Xiao, H., Wisniewski, J., Smith, M. M. and Wu, C. (2007). Nonhistone Scm3 and histones CenH3-H4 assemble the core of centromere-specific nucleosomes. *Cell* **129**, 1153-1164.
Moreno-Moreno, O., Torras-Llort, M. and Azorin, F. (2006). Proteolysis restricts localization of CID, the centromere-specific histone H3 variant of Drosophila, to centromeres. *Nucleic Acids Res.* **34**, 6247-6255.
Okada, M., Cheeseman, I. M., Hori, T., Okawa, K., McLeod, I. X., Yates, J. R., 3rd, Desai, A. and Fukagawa, T. (2006). The CENP-H-I complex is required for the efficient incorporation of newly synthesized CENP-A into centromeres. *Nat. Cell Biol.* **8**, 446-457.
Pandey, R., Heidmann, S. and Lehner, C. F. (2005). Epithelial re-organization and dynamics of progression through mitosis in Drosophila separase complex mutants. *J. Cell Sci.* **118**, 733-742.
Parks, A. L., Cook, K. R., Belvin, M., Dompe, N. A., Fawcett, R., Huppert, K., Tan, L. R., Winter, C. G., Bogart, K. P., Deal, J. E. et al. (2004). Systematic generation of high-resolution deletion coverage of the Drosophila melanogaster genome. *Nat. Genet.* **36**, 288-292.
Perpelescu, M., Nozaki, N., Obuse, C., Yang, H. and Yoda, K. (2009). Active establishment of centromeric CENP-A chromatin by RSF complex. *J. Cell Biol.* **185**, 397-407.
Pidoux, A. L., Choi, E. S., Abbott, J. K., Liu, X., Kagansky, A., Castillo, A. G., Hamilton, G. L., Richardson, W., Rappsilber, J., He, X. et al. (2009). Fission yeast Scm3: A CENP-A receptor required for integrity of subkinetochore chromatin. *Mol. Cell* **33**, 299-311.
Przewloka, M. R., Zhang, W., Costa, P., Archambault, V., D'Avino, P. P., Lilley, K. S., Laue, E. D., McAinsh, A. D. and Glover, D. M. (2007). Molecular analysis of core kinetochore composition and assembly in Drosophila melanogaster. *PLoS ONE* **2**, e478.
Santaguida, S. and Musacchio, A. (2009). The life and miracles of kinetochores. *EMBO J.* **28**, 2511-2531.
Schittenhelm, R. B., Heeger, S., Althoff, F., Walter, A., Heidmann, S., Mechtler, K. and Lehner, C. F. (2007). Spatial organization of a ubiquitous eukaryotic kinetochore protein network in Drosophila chromosomes. *Chromosoma* **116**, 385-402.
Schittenhelm, R. B., Chaleckis, R. and Lehner, C. F. (2009). Essential functional domains and intrakinetochore localization of Drosophila Spc105. *EMBO J.* **28**, 2374-2386.
Schuh, M., Lehner, C. F. and Heidmann, S. (2007). Incorporation of Drosophila CID/CENP-A and CENP-C into centromeres during early embryonic anaphase. *Curr. Biol.* **17**, 237-243.
Sonnichsen, B., Koski, L. B., Walsh, A., Marschall, P., Neumann, B., Brehm, M., Alleaume, A. M., Artelt, J., Bettencourt, P., Cassin, E. et al. (2005). Full-genome RNAi profiling of early embryogenesis in Caenorhabditis elegans. *Nature* **434**, 462-469.
Sugimoto, K., Kuriyama, K., Shibata, A. and Himeno, M. (1997). Characterization of internal DNA-binding and C-terminal dimerization domains of human centromere/kinetochore autoantigen CENP-C in vitro: role of DNA-binding and self-associating activities in kinetochore organization. *Chromosome Res.* **5**, 132-141.
Sun, X., Wahlstrom, J. and Karpen, G. (1997). Molecular structure of a functional Drosophila centromere. *Cell* **91**, 1007-1019.
Takahashi, K., Chen, E. S. and Yanagida, M. (2000). Requirement of Mis6 centromere connector for localizing a CENP-A-like protein in fission yeast. *Science* **288**, 2215-2219.
Talbert, P. B., Bryson, T. D. and Henikoff, S. (2004). Adaptive evolution of centromere proteins in plants and animals. *J. Biol.* **3**, 18.
Thibault, S. T., Singer, M. A., Miyazaki, W. Y., Milash, B., Dompe, N. A., Singh, C. M., Buchholz, R., Demsky, M., Fawcett, R., Francis-Lang, H. L. et al. (2004). A complementary transposon tool kit for Drosophila melanogaster using P and piggyBac. *Nat. Genet.* **36**, 283-287.
Torras-Llort, M., Moreno-Moreno, O. and Azorin, F. (2009). Focus on the centre: the role of chromatin on the regulation of centromere identity and function. *EMBO J.* **28**, 2337-2348.
Trazzi, S., Perini, G., Bernardoni, R., Zoli, M., Reese, J. C., Musacchio, A. and Della Valle, G. (2009). The C-terminal domain of CENP-C displays multiple and critical functions for mammalian centromere formation. *PLoS ONE* **4**, e5832.
Vagnarelli, P., Ribeiro, S. A. and Earnshaw, W. C. (2008). Centromeres: old tales and new tools. *FEBS Lett.* **582**, 1950-1959.
Van Hooser, A. A., Ouspenski, II, Gregson, H. C., Starr, D. A., Yen, T. J., Goldberg, M. L., Yokomori, K., Earnshaw, W. C., Sullivan, K. F. and Brinkley, B. R. (2001). Specification of kinetochore-forming chromatin by the histone H3 variant CENP-A. *J. Cell Sci.* **114**, 3529-3542.
Williams, J. S., Hayashi, T., Yanagida, M. and Russell, P. (2009). Fission yeast Scm3 mediates stable assembly of Cnp1/CENP-A into centromeric chromatin. *Mol. Cell* **33**, 287-298.
Winey, M., Mamay, C. L., O'Toole, E. T., Mastronarde, D. N., Giddings, T. H., Jr, McDonald, K. L. and McIntosh, J. R. (1995). Three-dimensional ultrastructural analysis of the Saccharomyces cerevisiae mitotic spindle. *J. Cell Biol.* **129**, 1601-1615.
Yang, C. H., Tomkiel, J., Saitoh, H., Johnson, D. H. and Earnshaw, W. C. (1996). Identification of overlapping DNA-binding and centromere-targeting domains in the human kinetochore protein CENP-C. *Mol. Cell. Biol.* **16**, 3576-3586.

Journal of Cell Science

Figure S1

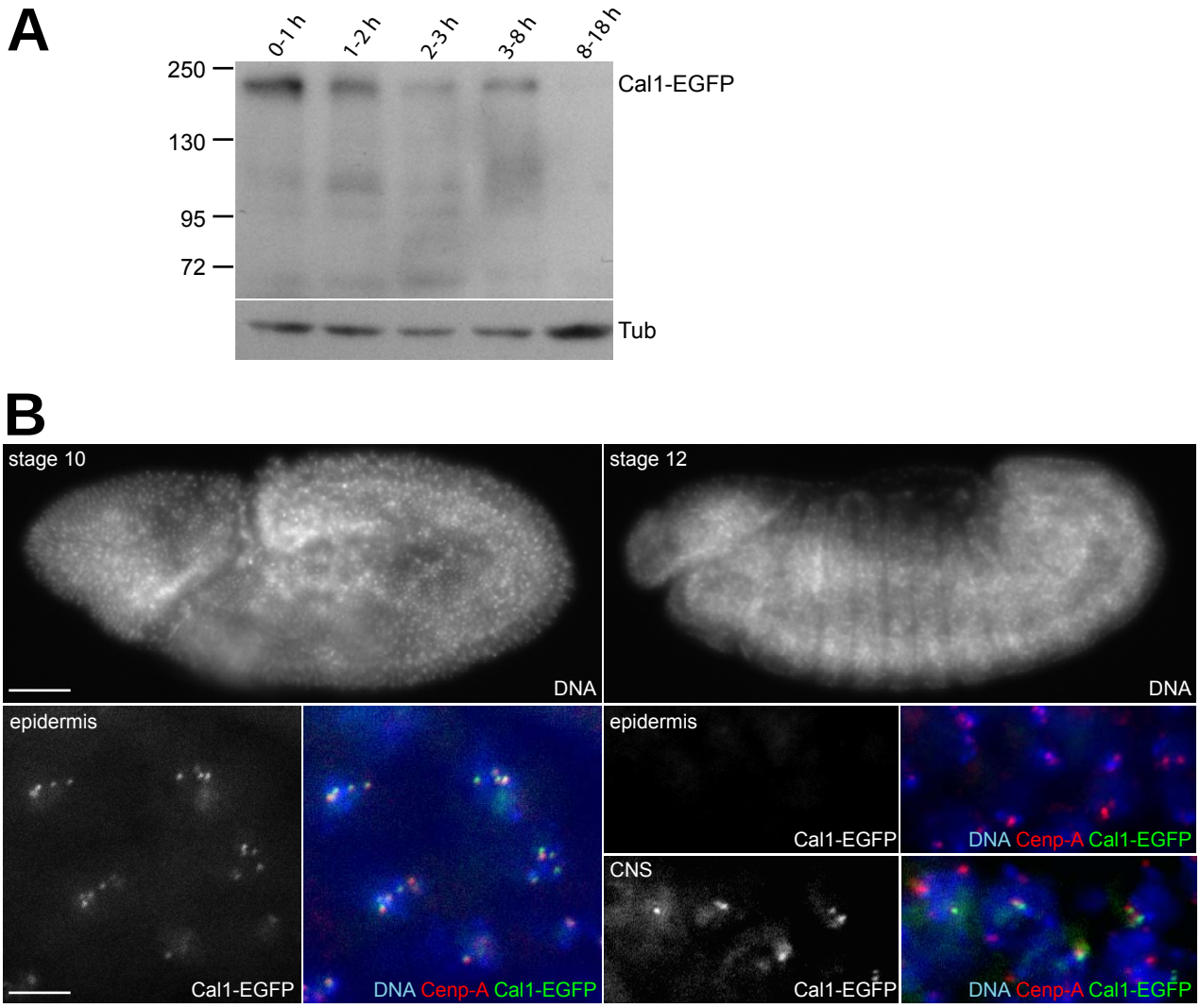

Figure S1. Cal1 expression during embryogenesis
(A) *gcal1-EGFP II.2* embryos were collected and aged as indicated above the lanes. Total embryo extracts were probed with anti-EGFP (Cal1-EGFP) and anti-α-tubulin (Tub), which served as a loading control. Migration of molecular weight markers (kDa) is indicated on the left side.
(B) *gcal1-EGFP II.2* embryos during stage 10 and 12 are shown in the left and right half, respectively, after double labeling with a DNA stain (DNA) and anti-Cenp-A/Cid (Cenp-A). High magnification views of regions from the epidermis or the central nervous system (CNS) are shown in the lower row, revealing Cal1-EGFP in mitotically proliferating cells but not in the post-mitotic epidermis at stage 12. Bars in the upper and lower row correspond to 60 and 5 µm, respectively.

Figure S2

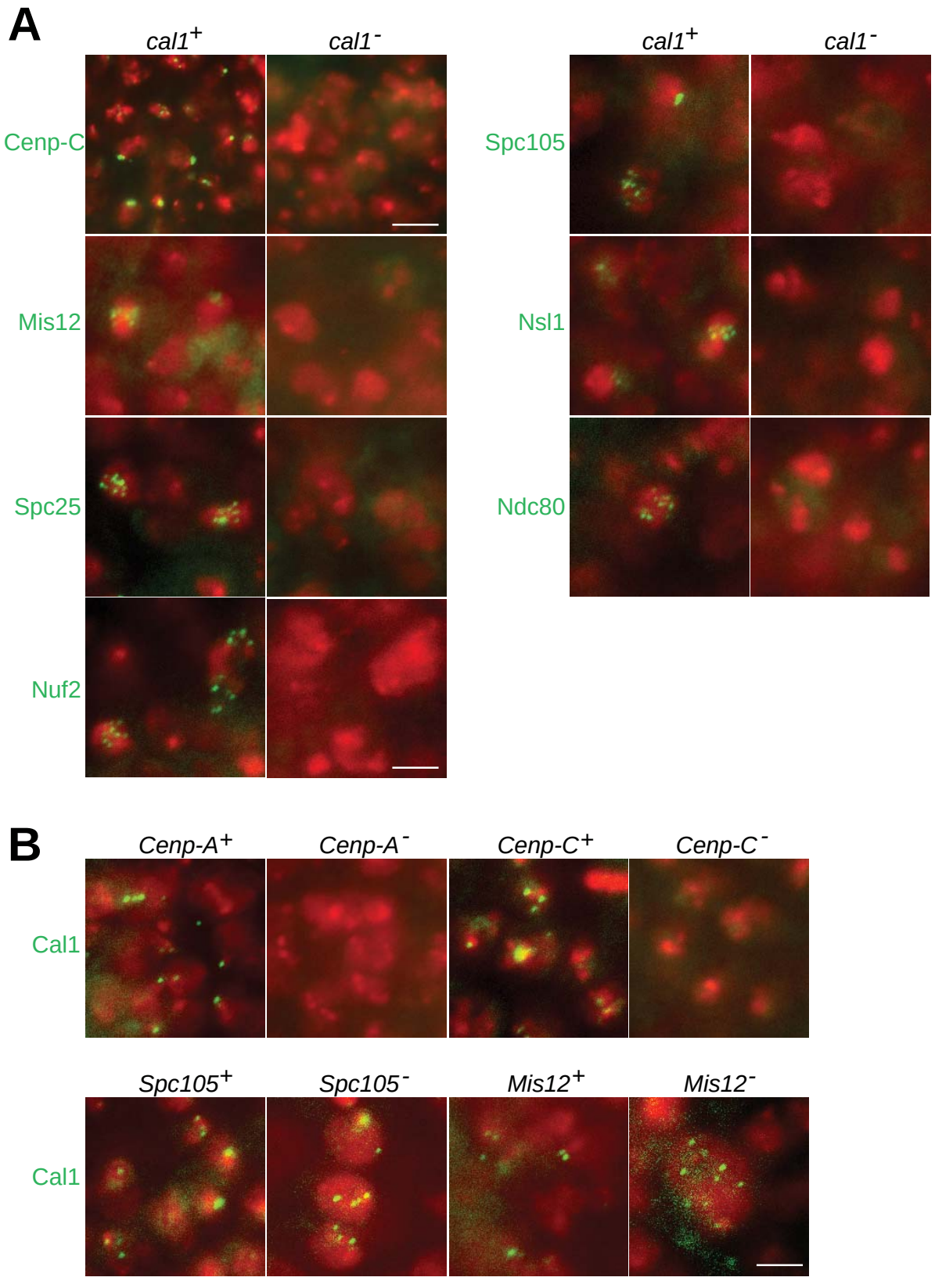
A
cal1+
cal1-
Cenp-C
Mis12
Spc25
Nuf2
cal1+
cal1-
Spc105
Nsl1
Ndc80
B
Cenp-A+
Cenp-A-
Cenp-C+
Cenp-C-
Cal1
Spc105+
Spc105-
Mis12+
Mis12-
Cal1

Figure S2. Cal1 acts at the top of the kinetochore assembly pathway.

(A) Localization of EGFP-fusions of Cenp-C, Spc105, Mis12, Nsl1, Spc25, Ndc80 and Nuf2 in homozygous *cal1*^{c03646} embryos (*cal1*$^{-}$) and in sibling control embryos (*cal1*$^{+}$) within the CNS after germband retraction. Representative mitotic figures are shown with the kinetochore proteins in *green* and DNA staining in *red*. Magnification in the first two Cenp-C panels is indicated by the upper bar = 6 μm; magnification in all other panels by the lower bar = 3 μm.

(B) Localization of Cal1-EGFP in *cid*$^{T12\text{-}1}$/*cid*$^{T22\text{-}4}$ (*Cenp-A*$^{-}$), *Cenp-C*^{prl41} (*Cenp-C*$^{-}$), *Spc105*^{1} (*Spc105*$^{-}$) and *Mis12*^{f03756} (*Mis12*$^{-}$) mutant embryos as well as in sibling control embryos (*Cenp-A*$^{+}$, *Cenp-C*$^{+}$, *Spc105*$^{+}$ and *Mis12*$^{+}$, respectively). Representative regions with Cal1-EGFP in *green* and DNA staining in *red* are shown at the stage where phenotypic abnormalities start in the mutant embryos, i.e. during mitosis 16 in *Cenp-C* and *Spc105* mutants and during the later mitotic divisions in the CNS in *Mis12* and *Cenp-A/cid* mutants. Bar = 3 μm.

Figure S3

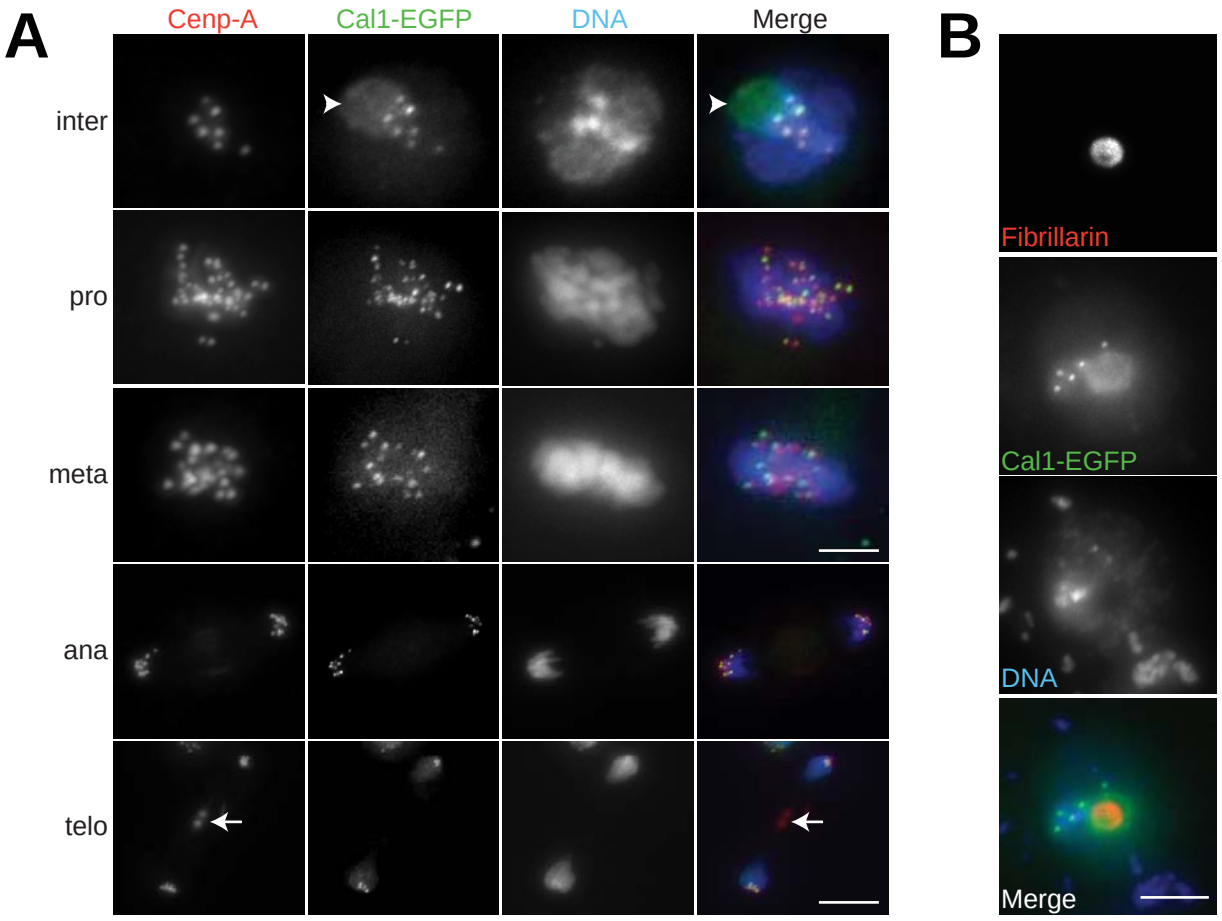

Figure S3. Intracellular localization of Cal1-EGFP
(A) Stably transfected S2R+ cells expressing Cal1-EGFP were double labeled with an antibody against Cenp-A/Cid (Cenp-A) and a DNA stain (DNA). Co-localization of Cal1-EGFP with Cenp-A/Cid at centromeres was observed throughout the cell cycle. In addition, Cal1-EGFP signals were also prominent in the nucleolus (arrowhead; see also B). The arrow indicates non-specific midbody staining by anti-Cenp-A/Cid. The bar in the third row illustrates magnification in the top three rows and corresponds to 5 µm; the bar in the bottom row illustrates magnification in the two bottom rows and corresponds to 7 µm.
(B) During interphase, Cal1-EGFP (Cal1-EGFP) is present in and around the nucleolus, as revealed by double labeling with an antibody against Fibrillarin (Fibrillarin) and DNA staining (DNA). Bar = 5 µm.

Figure S4

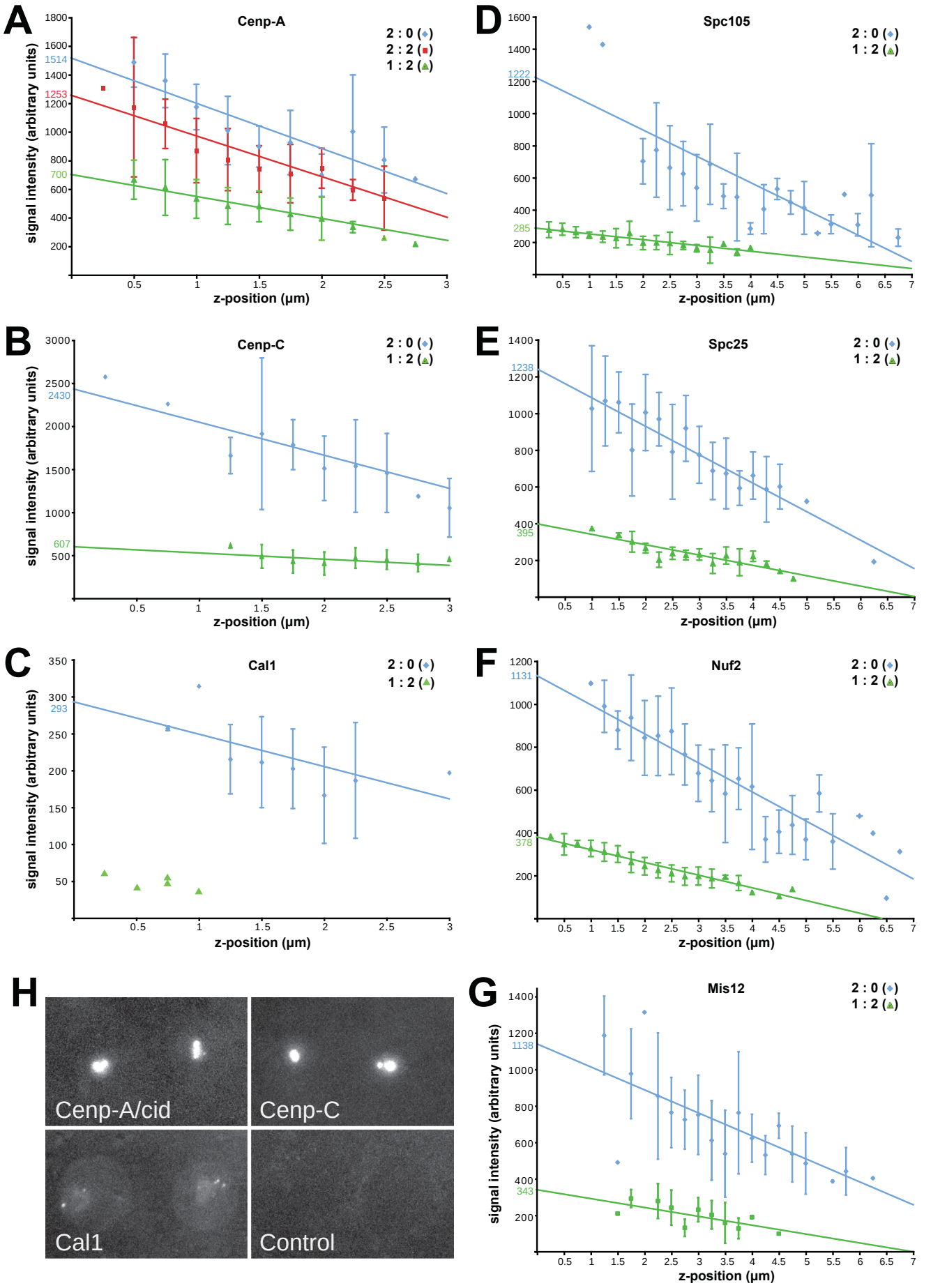
A
Cenp-A
2 : 0 (♦)
2 : 2 (■)
1 : 2 (▲)
signal intensity (arbitrary units)
z-position (µm)
1514
1253
700
B
Cenp-C
2 : 0 (♦)
1 : 2 (▲)
2430
607
C
Cal1
2 : 0 (♦)
1 : 2 (▲)
293
D
Spc105
2 : 0 (♦)
1 : 2 (▲)
1222
285
E
Spc25
2 : 0 (♦)
1 : 2 (▲)
1238
395
F
Nuf2
2 : 0 (♦)
1 : 2 (▲)
1131
378
G
Mis12
2 : 0 (♦)
1 : 2 (▲)
1138
343
H
Cenp-A/cid
Cenp-C
Cal1
Control

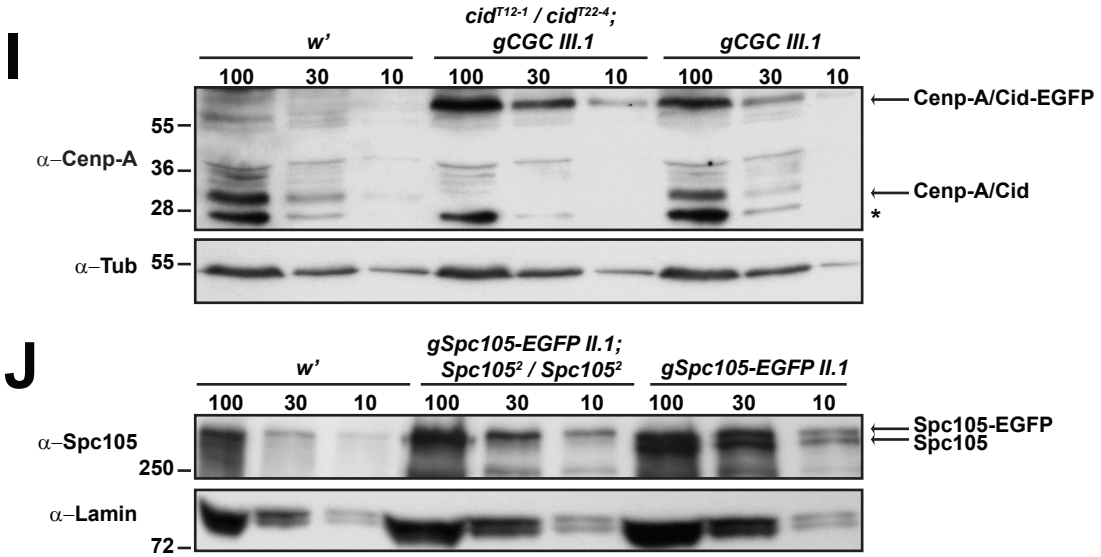

Figure S4. Stoichiometry of Drosophila centromere and kinetochore proteins.
(A-G) EGFP signal intensities observed in wing imaginal disc cells expressing EGFP fused to either the centromere proteins Cenp-A/Cid (A), Cenp-C (B) and Cal1 (C) or the kinetochore proteins Spc105 (D), Spc25 (E), Nuf2 (F) and Mis12 (G) were quantified and grouped according to their average focal depth. The average signal intensity (with s.d.) for each bin was plotted as a function of their z-position. Y intercepts of the linear regressions were used for comparisons of relative protein levels. To evaluate the accuracy of our quantifications, EGFP fusion proteins were expressed not only in a corresponding null mutant background but also in a background with functional endogenous genes. Untagged protein expressed from the endogenous genes is expected to compete with the EGFP-tagged protein and hence predicted to lower EGFP signal intensities at centromeres/kinetochores. Blue color represents data that was obtained with cells expressing two EGFP transgene copies and no functional endogenous copies (2:0), red color with cells expressing two EGFP transgene copies and two functional endogenous copies (2:2), and green color with cells expressing one EGFP transgene copy and two functional endogenous copies (1:2). In case of Cal1-EGFP, signals in the wild-type background were close to background and therefore difficult to detect, resulting in fewer data points which are shown individually as green triangles (C). Taking into account the observed relative expression levels of EGFP-tagged and untagged proteins (see also I and J) and assuming equal efficiency of incorporation into the centromere/kinetochore, the measured effects of competition deviate by less than 30% from the predicted competition effects.
(H) EGFP signals in live peripodial membrane cells of wing imaginal discs expressing either no EGFP (control) or EGFP fused to Cenp-A/Cid, Cenp-C or Cal1 in a corresponding null mutant background after identical acquisition and image processing (maximum projection). While Cal1-EGFP is detected not only at the centromere, but also in the nucleolus and weakly throughout the nucleus, strongly overexposed but exclusively centromeric signals are apparent in the case of Cenp-A/Cid-EGFP and Cenp-C-EGFP. Quantification of the Cal1-EGFP signals indicated that about 3.3% is centromeric, 21% nucleolar and 76% distributed throughout the nucleus (n = 5).
(I) Total extracts of 5-8 h old embryos (the exact genotypes are depicted above the lanes) were probed by immunoblotting with anti-Cenp-A/Cid (α-Cenp-A) and anti-α-Tubulin (α-Tub) to control for loading. The expression level of Cenp-A/Cid-EGFP was found to be approximately 3-fold higher than that of the endogenous Cenp-A/Cid, which explains the deviation between the expected and the observed centromeric incorporation of Cenp-A/Cid-EGFP in a null mutant compared to wild-type background (see also A). The numbers above the lanes indicate embryo equivalents loaded and the asterisk marks a prominent, unspecific band. The migration of the molecular weight marker (kDa) is indicated on the left side.
(J) Total extracts of 5-8 h old embryos (the exact genotypes are depicted above the lanes) were probed by immunoblotting with anti-Spc105 (α-Spc105) and anti-Lamin (α-Lamin), which served as a loading control. The expression levels of Spc105-EGFP and endogenous Spc105 were found to be similar, which is consistent with the observed decrease of centromeric incorporation of Spc105-EGFP in wild-type compared to null mutant background (see also D). The numbers indicate either embryo equivalents loaded (above the lanes) or the migration of the molecular weight marker (kDa; left side).

Figure S5

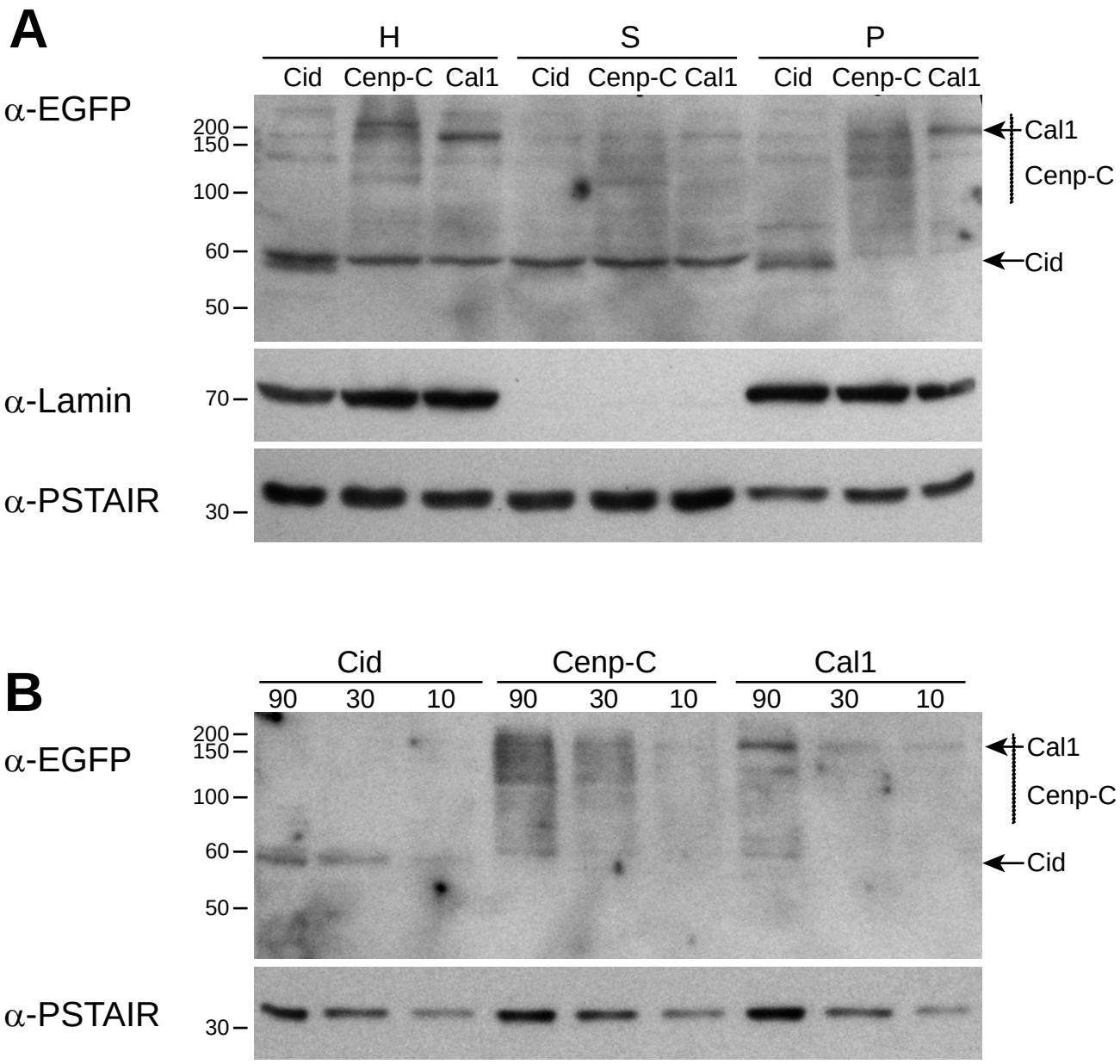

Figure S5. Expression levels EGFP fusion proteins of Cenp-A/Cid, Cenp-C and Cal1.
(A) Embryos were collected from strains with transgenes driving expression of EGFP fused to either Cenp-A/Cid, Cenp-C or Cal1 under control of the corresponding cis-regulatory regions in the corresponding null mutant backgrounds. 5-8 hour embryos were homogenized (H) followed by separation of a crude nuclear fraction (P) from the soluble material (S) by centrifugation. Immunoblotting with anti-EGFP (α-EGFP) was used to detect the different EGFP fusion proteins. Re-probing with anti-Lamin (α-Lamin) and anti-PSTAIR (α-PSTAIR) which reacts with Cdk1 was used to control the fractionation.
(B) For a comparison of expression levels, serial dilutions of crude nuclear fractions obtained from 90, 30, or 10 embryos, respectively, were immunoblotted with anti-EGFP (α-EGFP) and anti-PSTAIR (α-PSTAIR) as a loading control. Densitometric quantification indicated that the expression levels of Cenp-A/Cid-EGFP and Cal1-EGFP were 5.2 and 3.7 fold lower than that of Cenp-C-EGFP. Taking into account that only 3.3% of Cal1-EGFP is centromeric (Fig. S4H), this yields a stoichiometric ratio of centromeric Cenp-A/Cid, Cenp-C and Cal1 of about 20 : 100 : 0.9 compared to 60 : 100 : 1.9 obtained by purely microscopic EGFP signal detection and quantification (Table 1, Fig. 4C, Fig. S4A-C).

Figure S6

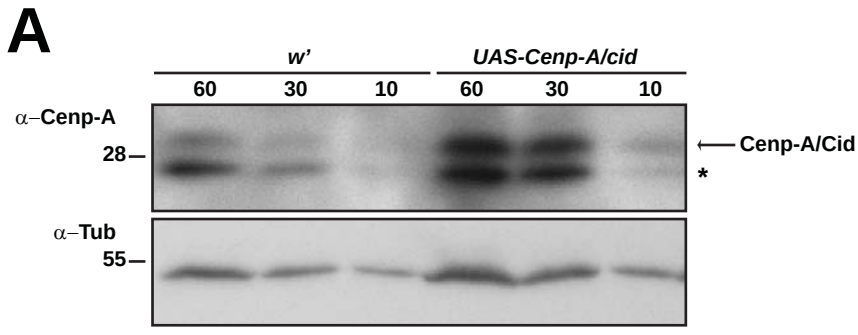
A
w'
UAS-Cenp-A/cid
60
30
10
60
30
10
α–Cenp-A
28
Cenp-A/Cid
*
α–Tub
55

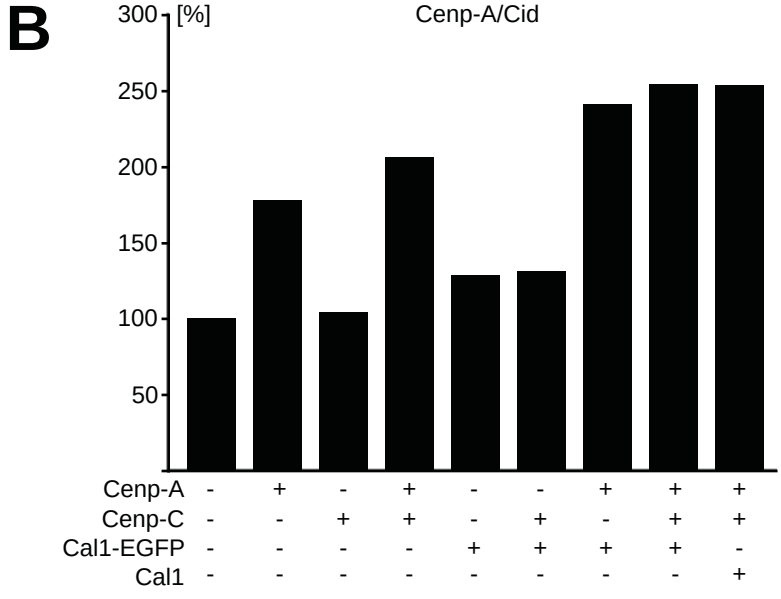
B
Cenp-A/Cid
[%]
300
250
200
150
100
50
Cenp-A - + - + - - + + +
Cenp-C - - + + - + - + +
Cal1-EGFP - - - - + + + + -
Cal1 - - - - - - - - +

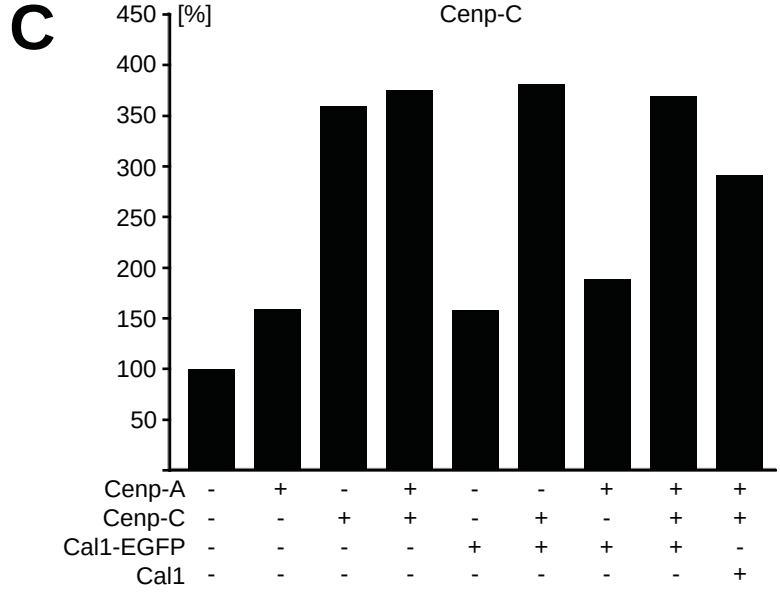
C
Cenp-C
[%]
450
400
350
300
250
200
150
100
50
Cenp-A - + - + - - + + +
Cenp-C - - + + - + - + +
Cal1-EGFP - - - - + + + + -
Cal1 - - - - - - - - +

Figure S6. Levels of overexpression of Cenp-A/Cid and Cenp-C in *Drosophila* embryos.

(A) Total extracts of 5-8 h old w^1 embryos and embryos overexpressing paternally derived *UAS-Cenp-A/cid* driven by maternal *α4tub-GAL4-VP16* were probed with anti-Cenp-A/Cid (α-Cenp-A) and anti-α-Tubulin (α-Tub), which served as loading control. The numbers indicate loading in embryo equivalents (above the lanes) or the position of molecular weight marker (kDa; left side). The asterisk marks a prominent, unspecific band.

(B and C) Paternally derived *UAS-Cenp-A/cid*, *UAS-Cenp-C* and *UAS-cal1-EGFP* or *UAS-cal1* were expressed individually or in combinations using maternal *α4tub-GAL4-VP16*. Total extracts were prepared and analyzed by immunoblotting as illustrated in panel A. The band intensities obtained with anti-Cenp-A/Cid (B) and anti-Cenp-C (C) were quantified (see Materials and Methods). The band intensity observed in the w^1 control embryos was set to 100%. The type(s) of *UAS* transgene expressed is indicated below the bars.

Figure S7

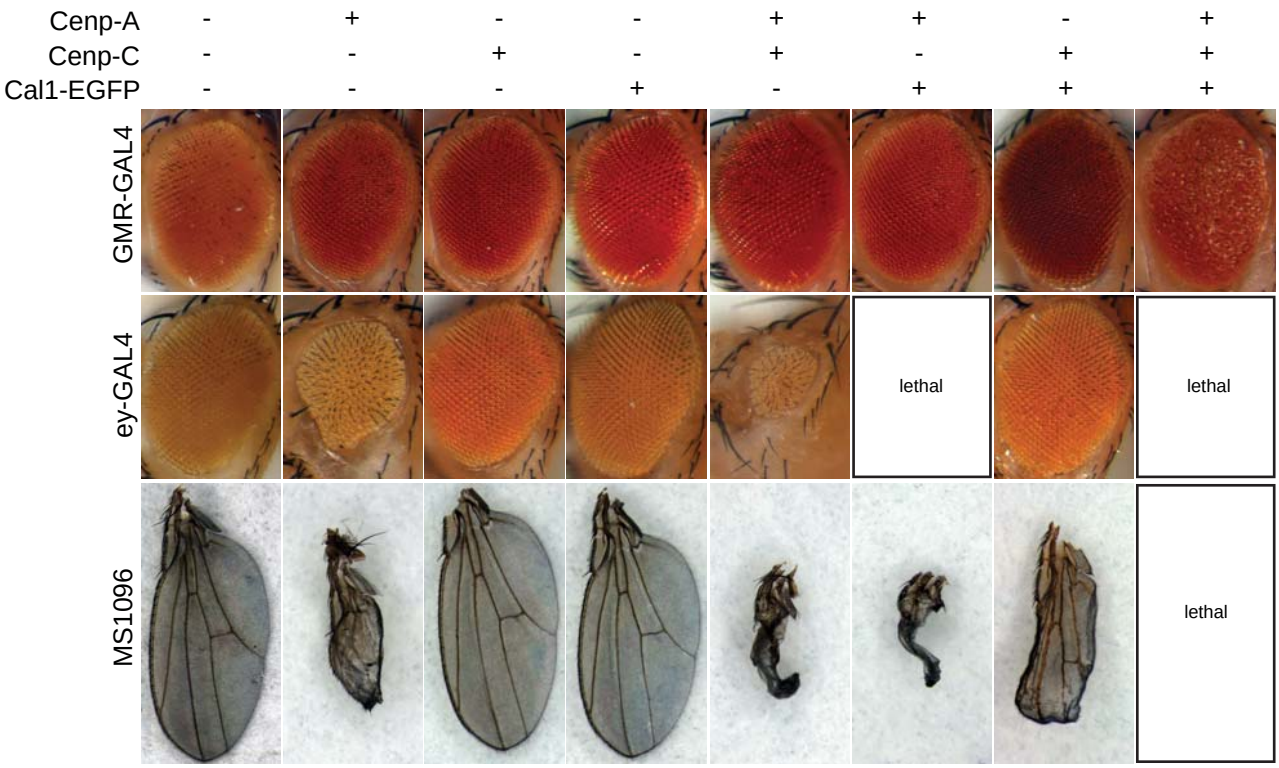

Figure S7. Synergistic effects of co-overexpression of Cenp-A/Cid, Cenp-C and Cal1 during eye and wing development.
The drivers *GMR-GAL4*, *ey-GAL4* or *MS1096* were used to express various *UAS* target transgenes (as indicated on top of the images) during eye and wing development. Wild-type eyes and wings were present in control flies with only one copy of one of these GAL4 driver transgenes and no *UAS* target transgenes. When *GMR-GAL4* as well as *UAS-Cenp-A/cid*, *UAS-Cenp-C* and *UAS-cal1-EGFP* were all present, an aberrant eye phenotype was observed. In contrast, the combination of *GMR-GAL4* with either double combinations or single *UAS* target transgenes did not result in aberrant phenotypes. In case of *ey-GAL4* and *MS1096*, expression of *UAS-Cenp-A/cid* alone already led to aberrant eye and wing phenotypes. In combination with *UAS-cal1-EGFP* or *UAS-Cenp-C*, these phenotypes became stronger, and overexpression of all three *UAS* target transgenes resulted in lethality.

Figure S8

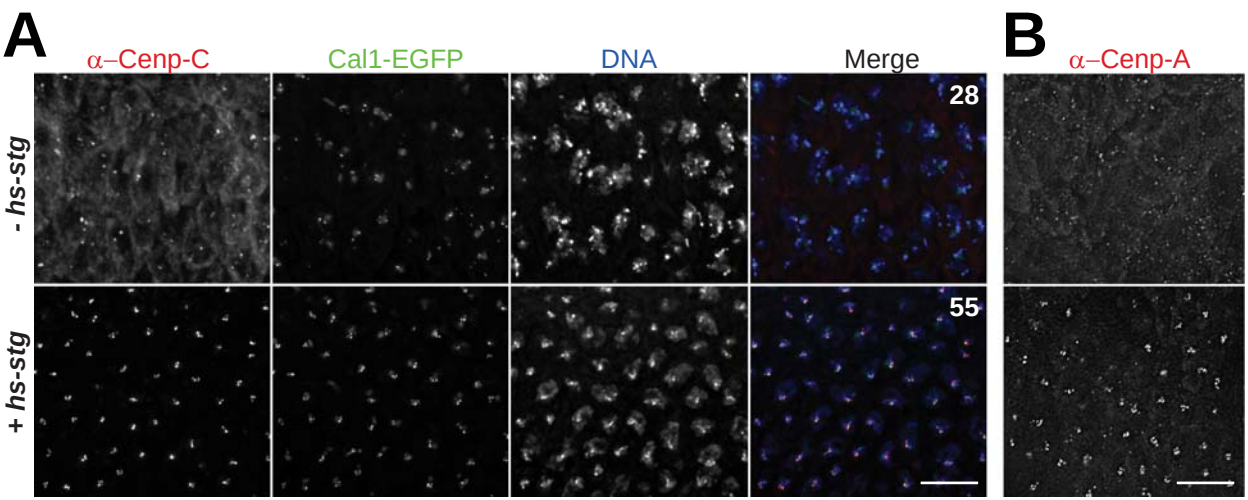

Figure S8. The increase in centromere protein levels after co-overexpression of Cenp-A/Cid, Cenp-C and Cal1 depends on progression through mitosis.
UAS-cal1-EGFP, *UAS-Cenp-A/cid* and *UAS-Cenp-C* were co-expressed ubiquitously in *string* (*stg*) mutant embryos in which a heat-inducible *stg* transgene was either absent (top row, -*hs-stg*) or present (bottom row, +*hs-stg*). 4-5 h old embryos were exposed to a heat shock (15 minutes at 37°C) followed by recovery (30 minutes at 25°C) and labeling with either anti-Cenp-C (A, α-Cenp-C) or with anti-Cenp-A/Cid (B, α-Cenp-A), as well as with a DNA stain (DNA) and anti-β-galactosidase for genotype determination (not shown). The number of nuclei present within the displayed regions is indicated in the merged panels. These numbers as well as the size of the nuclei demonstrate that *hs-stg* expression forces progression through a successful mitosis, while in the absence of *hs-stg* cells remain arrested in G2 (Edgar and O'Farrell, 1990). Increased levels of centromeric anti-Cenp-C and anti-Cenp-A/Cid labeling were only detected after progression through the *hs-stg*-induced mitosis. Bar = 10 μm.